ROSAT PSPC OBSERVATIONS OF CL0016+16

NASA Grant NAG5-2156

Annual Report 1, 2 and 3

For the Period 15 December 1992 through 14 December 1995

Principal Investigator
Dr. John P. Hughes

April 1996

Prepared for:

National Aeronautics and Space Administration
Goddard Space Flight Center
Greenbelt, Maryland 20771

Smithsonian Institution
Astrophysical Observatory
Cambridge, Massachusetts 02138

The Smithsonian Astrophysical Observatory
is a member of the
Harvard-Smithsonian Center for Astrophysics

The NASA Technical Officer for this grant is Dr. Robert Petre, Code 666, Laboratory for High Energy Astrophysics, Space Science Directorate, Goddard Space Flight Center, Greenbelt, Maryland 20771.

NASA grant NAG5-2156 has supported the analysis of several *ROSAT* observations, which have resulted in the following publications, copies of which are also attached.

1.) X-Ray Observations of the Sunyaev-Zel'dovich Decrement Clusters Abell 665 and CL0016+16," J. P. Hughes, and M. Birkinshaw, Proceedings of the 37th Yamada Conference, *Evolution of the Universe and its Observational Quest*, ed., K. Sato, in press.

2.) "Complex Spatial Structures in Sunyaev-Zel'dovich Decrement Clusters Abell 665 and CL0016+16," J. P. Hughes, and M. Birkinshaw, *The Soft X-Ray Cosmos*, ROSAT Science Symposium, AIP Conference Proceedings 313, eds., E. M. Schlegel & R. Petre, 378, (1994).

3.) "Discovery of Be/X-ray Stars in Two Supernova Remnants in the Small Magellanic Cloud," J. P. Hughes and R. C. Smith, *Astronomical Journal*, **107**, 1363, (1994).

4.) "A New Transient Pulsar in the Small Magellanic Cloud with an Unusual X-ray Spectrum," J. P. Hughes, *Astrophysical Journal (Letters)*, **427**, L25, (1994).

5.) "A New X-Ray–Discovered Cluster of Galaxies Associated with CL0016+16," J. P. Hughes, M. Birkinshaw, and J. P. Huchra, *Bull. Amer. Astr. Soc.*, **26**, 1395, (1994).

6.) "A New X-ray–Discovered Cluster of Galaxies Associated with CL0016+16," J. P. Hughes, M. Birkinshaw, and J. P. Huchra, *Astrophysical Journal (Letters)*, **448**, L93, (1995).

7.) "The Distance to CL0016+16 and the Hubble Constant," J. P. Hughes, and M. Birkinshaw, *Bull. Amer. Astr. Soc.*, **27**, 1292, (1995).

8.) "The Expansion of the X-Ray Remnant of Tycho's Supernova (SN1572)," J. P. Hughes, in the Proceedings of the International Conference on X-Ray Astronomy – *ASCA* 3rd Anniversary – *X-Ray Imaging and Spectroscopy of Cosmic Hot Plasmas*, in press.

Proceedings of the 37th Yamada Conference held June 8-12, 1993, Tokyo, Japan
Evolution of the Universe and its Observational Quest

X-RAY OBSERVATIONS OF THE SUNYAEV-ZEL'DOVICH DECREMENT CLUSTERS ABELL 665 AND CL0016+16

John P. HUGHES and Mark BIRKINSHAW
Harvard-Smithsonian Center for Astrophysics, 60 Garden Street, Cambridge, MA 02138 USA

Abstract

We report on our analysis of deep X-ray observations of Abell 665 and CL0016+16 obtained by the ROSAT position sensitive proportional counter (PSPC) as part of a project to characterize the density and temperature structure of clusters with well-measured Sunyaev-Zel'dovich decrements. The X-ray images of both clusters show dramatic departures from the standard single-component hydrostatic isothermal-β model.

1. Analysis

A665 was observed by the PSPC in April 1991 for 38641 s. Fig. 1a shows an X-ray map of the cluster after the data were background subtracted, exposure corrected, and adaptively smoothed. The structure of the cluster is complex. There is a main component extending to a radius of 8′. Near the center of this component, but offset from it by about 1′, is a smaller and brighter, but clearly extended, second component. Numerous point sources, nearly all of which remain unidentified at this time, appear in the field as well.

Maximum-likelihood fits to the raw two-dimensional image data were carried out. Point sources in the outskirts of the cluster were excluded from the fits. Two isothermal-β models with parameter values $\beta = 0.85$, $R_c = 2.7'$ and $\beta = 1.24$, $R_c = 0.9'$ were clearly required as was a previously unrecognized point source near the core of the second component. The residuals from this fit showed the presence of two additional surface brightness features each seemingly associated with a cluster component. These features were modeled as prolate spheroids of hot gas. In total five spatial components were required for a good fit.

PSPC X-ray spectra were extracted from 2 separate regions of the cluster: one dominated by the smaller subcluster and the other by the main component. In the fits each PSPC spectrum was allowed to have an independent thermal model, while the sum was required to fit the *Ginga* and *Einstein* IPC data (Hughes & Tanaka 1992). The best fit was found for roughly equal temperatures and a column density consistent with the Galactic value. We can

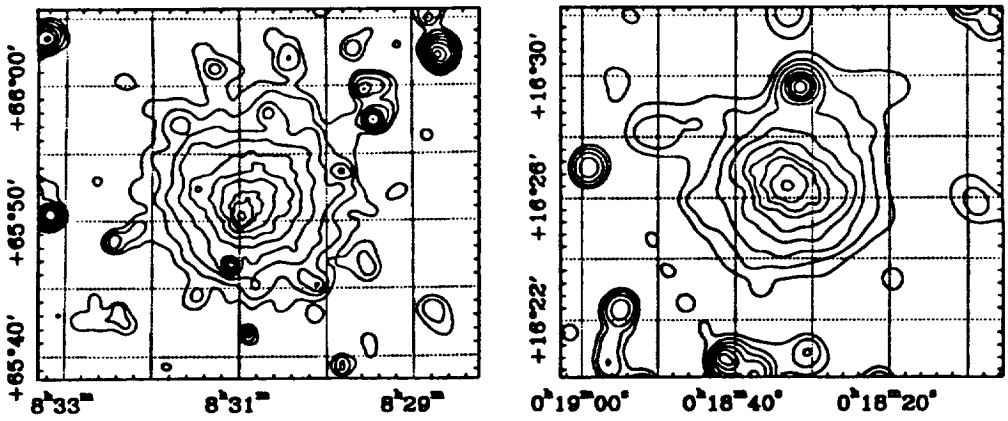

Fig. 1. (a) Left: ROSAT PSPC X-ray map of Abell 665. Contours are logarithmically spaced from 0.25% to 90% of the peak value. (b) Right: ROSAT PSPC X-ray map of CL0016+16. Contours are logarithmically spaced from 0.5% to 90% of the peak value.

set a strong lower limit to the temperature of either component: $kT > 5$ keV, which rules out the presence of an active cooling flow.

The cluster CL0016+16 was observed by the ROSAT PSPC in July 1992 for 43157 s. Fig. 1b shows a map of the cluster's X-ray emission after background subtraction, exposure correction, and adaptive smoothing. The structure of this cluster is also quite complex.

We performed elliptical isophotal analysis on the smoothed data. The ellipticity increases from 0 near the cluster center to a maximum of 0.24 at a radius of 80″ before decreasing to 0 again at 120″. Over this radial range the position angle of the major axis is roughly constant at 50°, but at 120″ this position angle changes abruptly by nearly 90°. From 120″ to 200″ the ellipticity is in the range 0.05 to 0.1.

2. Conclusions

Abell 665 clearly shows two subclusters in the process of merging. This is supported by the large β value (of 1.24) for the smaller, merging, component, which indicates a steep radial fall-off in its gas density. We believe the ellipsoidal clouds found in our image analysis to be the remnants of the gas stripped off the outer atmosphere of the subcluster during a passage through the core of the main component. These observations are in excellent agreement with recent numerical simulations of the merger of a dominant cluster and a small subcluster (Roettiger, Burns, & Loken 1993).

We interpret the X-ray structure of CL0016+16 in a similar manner. Here however, we believe that the strong ellipticity seen at 80″ is caused by the continuing merger of two nearly equal components. The distribution of galaxies (Dressler and Gunn 1992), which clearly shows a bimodal spatial structure, is strongly supportive of this picture.

3. References

1. Dressler, A. and Gunn, J. E., 1992, *Ap. J. Suppl.*, **78**, 1.
2. Hughes, J. P. and Tanaka, Y., 1992, *Ap. J.*, **398**, 62.
3. Roettiger, K., Burns, J. and Loken, C., 1993, *Ap. J.*, **407**, L53.

(2)

AIP CONFERENCE PROCEEDINGS 313

THE SOFT X-RAY COSMOS

ROSAT SCIENCE SYMPOSIUM

COLLEGE PARK, MD NOVEMBER 1993

EDITORS: ERIC M. SCHLEGEL
NASA/GODDARD SPACE FLIGHT CENTER
AND
UNIVERSITIES SPACE RESEARCH ASSOCIATION

ROBERT PETRE
NASA/GODDARD SPACE FLIGHT CENTER

AIP PRESS

American Institute of Physics **New York**

COMPLEX SPATIAL STRUCTURES IN SUNYAEV-ZEL'DOVICH DECREMENT CLUSTERS ABELL 665 AND CL0016+16

John P. Hughes and Mark Birkinshaw
Harvard-Smithsonian Center for Astrophysics
60 Garden Street, Cambridge, MA 02138

Email ID
jph@cfa.harvard.edu, mb1@cfa.harvard.edu

ABSTRACT

We report on our analysis of deep X-ray observations of Abell 665 and CL0016+16 obtained by the ROSAT position sensitive proportional counter (PSPC) as part of a project to characterize the density and temperature structure of clusters with well-measured Sunyaev-Zel'dovich decrements. The X-ray images of both clusters show dramatic departures from the standard single-component hydrostatic isothermal-β model.

1. Analysis

The PSPC observed A665 in April 1991 for 38641 s. Fig. 1a shows the 0.4–2.4 keV band X-ray map of the cluster after the data were background subtracted, exposure corrected, and adaptively smoothed. The structure of the cluster is complex. The main cluster component extends to a radius of $8'$. Near its center, but offset from it by about $1'$, is a smaller and brighter, but clearly extended, second component. Numerous point sources, nearly all of which remain unidentified at this time, also appear in the field.

Maximum-likelihood fits to the raw two-dimensional image data were carried out. Two isothermal-β models, with parameter values $\beta = 0.85$, $R_c = 2.7'$ and $\beta = 1.24$, $R_c = 0.9'$, were clearly required, as was a previously unrecognized point source near the core of the second component. The residuals from this fit showed the presence of two additional surface brightness features each seemingly associated with a cluster component. These features were modeled as prolate spheroids of hot gas. In total five spatial components were required for a good fit. Spatially resolved PSPC X-ray spectroscopy showed that the 2 cluster components were consistent with having the same temperatures. Furthermore, it was possible to set a strong lower limit on the temperature of either component: $kT > 5$ keV, ruling out the presence of an active cooling flow.

The cluster CL0016+16 was observed by the PSPC in July 1992 for 43157 s. Fig. 1b shows a map of the cluster's 0.4–2.4 keV band X-ray emission after processing as above. The structure of this cluster is also complex. We performed elliptical isophotal analysis on the smoothed data. The ellipticity increases from 0 near the cluster center to a maximum of 0.24 at a radius of $80''$ before decreasing to 0 again at $120''$. Over this radial range the position angle of the major axis is roughly constant at 50°, but at $120''$ it changes abruptly by nearly 90°. From $120''$ to $200''$ the ellipticity is in the range 0.05 to 0.1. The derived positions of the ellipse centers vary with radius by less than $\sim 5''$.

The distribution of galaxies (Dressler and Gunn 1992), as well as data on gravitationally lensed arcs in CL0016+16 (Ellis 1993), shows a bimodal spatial structure. We found that the galaxy distribution is consistent with 2 nearly

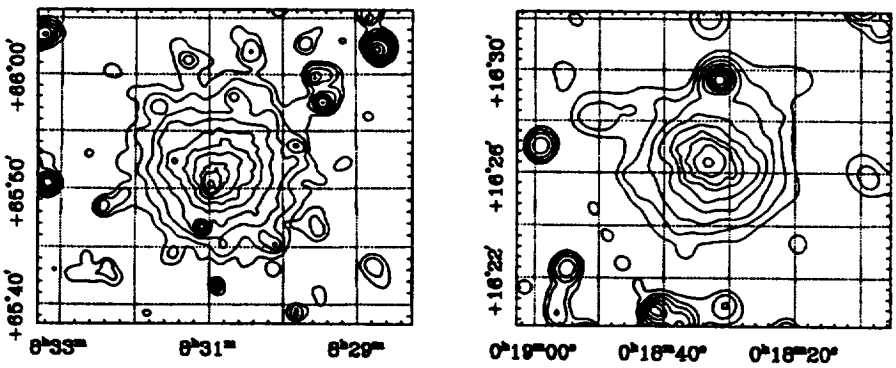

Fig. 1 (a) Left: ROSAT PSPC X-ray map of Abell 665. Contours are logarithmically spaced from 0.25% to 90% of the peak value. (b) Right: ROSAT PSPC X-ray map of CL0016+16. Contours are logarithmically spaced from 0.5% to 90% of the peak value.

equal mass groupings, separated by some 90″, and lying on either side of the bright central core of the X-ray image. When a similar two-component model for the gas distribution was fit to the X-ray data, the derived positions, separation, and relative intensities of the components were significantly different from the galaxian values. In particular the X-ray image appears to be dominated by a β-model component centered near the X-ray peak, between the 2 galaxy groupings.

2. Conclusions

A665 shows two subclusters in the process of merging. This is supported by the large β value (of 1.24) for the smaller, merging, component, which indicates a steep radial fall-off in its gas density. We believe the ellipsoidal clouds found in our analysis to be the remnants of the gas stripped off the outer atmosphere of the subcluster during a passage through the core of the main component. These observations agree well with numerical simulations of the merger of a dominant cluster and a small subcluster (Roettiger, Burns, & Loken 1993).

The optical data for CL0016+16 strongly support a scenario in which we are viewing this cluster as it undergoes a merger of two nearly equal components. At some level, this is supported by the strong ellipticity seen at ~80″ in the X-ray image. However, the presence of a single central X-ray surface brightness peak indicates that the gas distribution is more complex than just the superposition of two isothermal-β components: *e.g.*, the core might contain an unresolved point source or even a cooling flow. Additional study of the gas and galaxy distributions using the commmon cluster gravitational potential as the starting point should clarify these issues.

3. References

Dressler, A., & Gunn, J. E. 1992, ApJS, 78, 1

Ellis, R. 1993, Proceedings of the 37th Yamada Conference, *Evolution of the Universe and its Observational Quest*, ed., K. Sato, in press.

Roettiger, K., Burns, J., & Loken, C. 1993, ApJ, 407, L53

Harvar hsonian
Center f tophysics

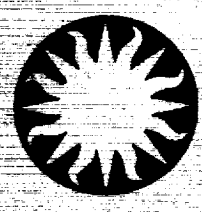

(Re)

DISCOVERY OF Be/X-RAY ... SUPERNOVA REMNANTS IN THE SM... NIC CLOUD

Harvard-Sm... Astrophysics

Departme... University

Cerro-To... Observatory

HARVARD COLLEGE OBSERVATORY

60 Garden St...

SMITHSONIAN ... ASTROPHYSICAL OBSERVATORY

...bridge, MA 02138

... OBSERVATORY

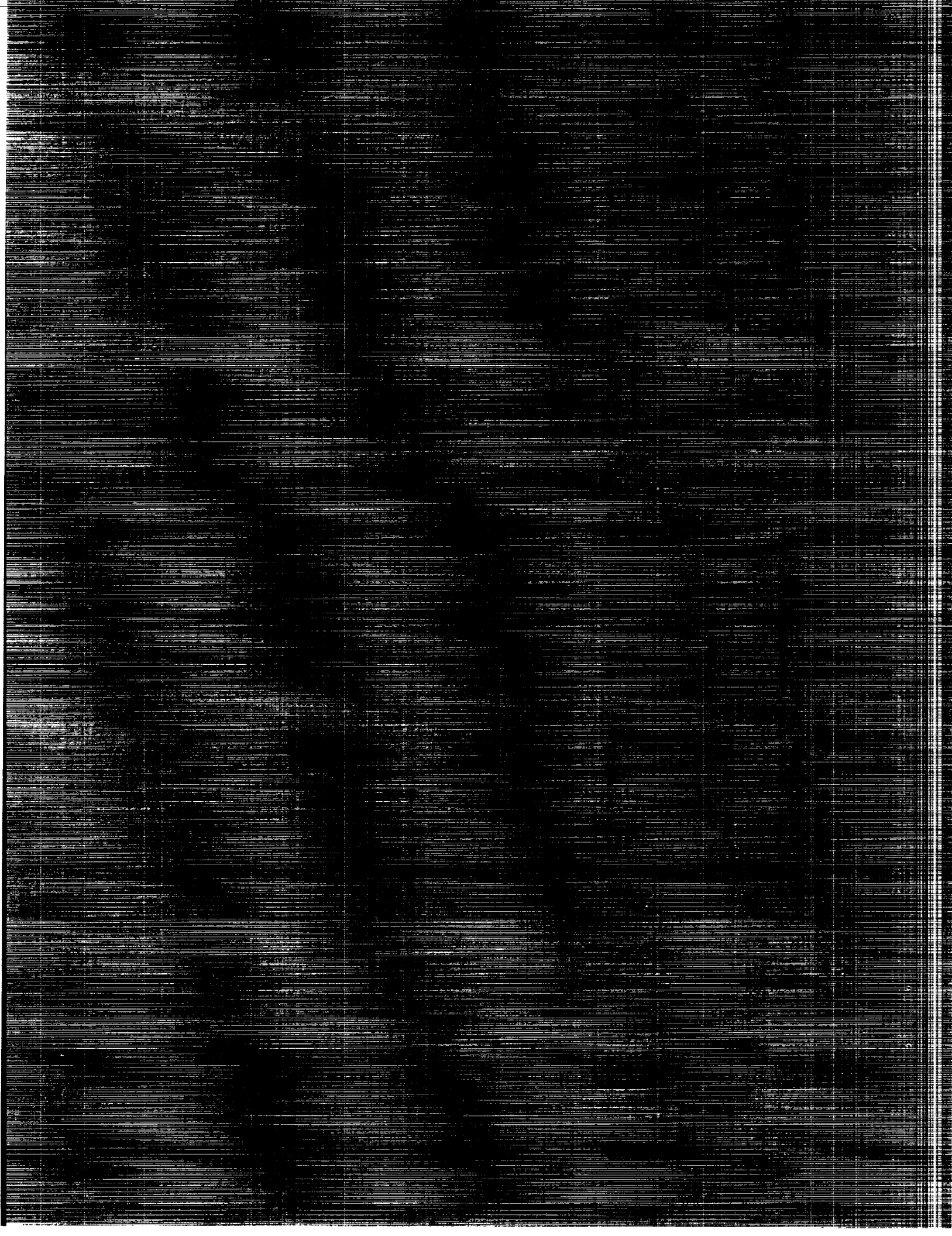

Center for Astrophysics
Preprint Series No. 3766

Discovery of Be/X-ray Stars in Two Supernova Remnants in the Small Magellanic Cloud

John P. Hughes[1]
Harvard-Smithsonian Center for Astrophysics
60 Garden Street, Cambridge, MA 02138, U.S.A.
Electronic-mail: jph@cfa.harvard.edu
and
Department of Physics, Kyoto University

and

R. Chris Smith
Cerro-Tololo Inter-American Observatory
Casilla 603, 1353 La Serena, Chile
Electronic-mail: csmith@noao.edu

To appear in *The Astronomical Journal*
April 1994

Received: 13 September 1993
Accepted: 17 December 1993

[1] Visiting Astronomer, Cerro-Tololo Inter-American Observatory, National Optical Astronomy Observatories, operated by the Association of Universities for Research in Astronomy, Inc., under contract with the National Science Foundation.

ABSTRACT

We present ROSAT high resolution X-ray images of two previously catalogued supernova remnants in the Small Magellanic Cloud (SMC): 0101−72.4 and 0104−72.3. These remnants were known to show optical, X-ray, and radio emission based on earlier observations: the present data show the first evidence for arcsecond-scale X-ray structure. There is no diffuse X-ray emission associated with the optically emitting shell in 0101−72.4; we set a 3σ upper limit of 7×10^{34} erg s^{-1} on the 0.2–2 keV luminosity from the region. The X-ray emission comes instead from a weak point-like object near the limb of the remnant. Optical observations of this source reveal a $m_V = 14.8$ blue star with Hα and Hβ in emission; we identify this as a Be star in the SMC. No evidence for variability down to timescales of about 1 second was found in the ROSAT data; however, a comparison of the ROSAT and *Einstein* fluxes indicates possible long term variability by a factor of $\sim$2 over several years. The other SNR, 0104−72.3, also contains a point-like X-ray source with a blue optical counterpart ($m_V = 16.7$) and Hα emission. We tentatively identify this as a Be star as well. In addition to the point source there is weak diffuse X-ray emission from 0104−72.3 ($L_X \sim 1.4 \times 10^{35}$ erg s^{-1}), but the remnant's appearance in the X-ray band is considerably different from that in either the radio or optical band. We argue for a physical association between the SNRs and Be/X-ray stars. A large space velocity ($\gtrsim 100$ km s^{-1}) for the Be/X-ray binaries is required if the explosions that produced the remnants also formed the neutron stars in the binaries. Alternatively, the associations could be the result of common membership in OB associations in the SMC.

1. INTRODUCTION

It is widely believed that compact objects (neutron stars and black holes) are produced in the same supernova explosions which give rise to the often beautiful shells of expanding gas known as supernova remnants (SNRs). However the direct observational connection between the two types of remnants (compact and gaseous) is much more tenuous. There are only a handful of cases in which a compact object can be reliably associated with the SN explosion which formed it; the Crab pulsar being the most famous example. In total, there are less than 20 cases where a compact object is observed or inferred to exist in association with a SNR (Lang 1992) and in most of these the compact object is an isolated pulsar. In this work we report on the discovery of 2 compact objects associated with SNRs in the Small Magellanic Cloud (SMC) based on observations made with the ROSAT satellite. These are of particular interest because they are among the first examples of Be/X-ray stars associated with SNRs.

Be/X-ray stars are binary systems consisting of a neutron star in a wide and (usually) eccentric orbit about a rapidly rotating Be star (see White 1989, and references within). The X-ray emission arises from the accretion of matter onto the neutron star via a quasi-steady wind from the Be star. Persistent X-ray emission from these sources is usually at a level of $\sim 10^{34}$ erg s^{-1}. However, due to orbital eccentricity and the likely possibility of episodic mass loss from the Be star, such systems are often highly variable X-ray sources and outbursts up to 10^4 times the quiescent level are possible. The Be phenomena is not directly related to the X-ray emission but rather arises from a rotationally-induced disk of material around the B star which gives rise to the prominent Balmer line emission features seen in the optical spectrum.

We obtained X-ray images of several SNRs with the ROSAT Observatory. The ROSAT mission (Trümper 1983) consists of a high resolution grazing incidence X-ray telescope (XRT) (Aschenbach 1988) with two types of focal plane instruments: a position sensitive proportional counter (PSPC) (Pfeffermann *et al.* 1986) and a high resolution imager (RHRI) (Zombeck *et al.* 1990). In this paper we utilize data from both ROSAT focal plane instruments. The RHRI observations were carried out between 9 November and 10 December 1991 for an exposure time of 20165 s and the PSPC observed this region of the sky for 4909 s on 12 - 13 May 1993. The prime target of both observations was the brightest SNR in the X-ray band in the SMC, 0102−72.2, an unusual remnant showing emission from high velocity oxygen-rich ejecta, which will be discussed elsewhere (Hughes 1994). The current article presents results for two other known SNRs which happened to lie in this field: 0101−72.4 and 0104−72.3. At the off-axis positions of these sources (8.5′ and 10.4′, respectively) the imaging performance of the ROSAT XRT/HRI, as represented by the 50% encircled energy radius, is 5.4″ and 7.6″, somewhat larger than the measured on-axis value of 3″ (David *et al.* 1992), but certainly adequate for detecting point sources. Both SNRs lay within the central region of the PSPC, as defined by the circular window

support ring. The ROSAT PSPC and HRI standard processing systems detected both SNRs.

Mathewson *et al.* 1983 presented the first optical image of 0101−72.4. It shows an incomplete shell with a mean optical diameter of 24 pc (throughout this paper we use a distance to the SMC of 57.5 kpc, van den Bergh 1989) and a slightly smaller size (∼18 pc) in the radio. The optical and radio images of 0104−72.3 (Mathewson *et al.* 1984) show a filamentary structure with a mean size of ∼26 pc but there is no obvious shell. The X-ray luminosities of both remnants determined by the *Einstein* imaging proportional counter (IPC) in the 0.15–4.5 keV band were moderately low: 5×10^{35} (0101−72.4) and 3.4×10^{35} (0104−72.3) erg s^{-1}, especially in comparison to similar size remnants in the Large Magellanic Cloud (LMC). In this paper we present the first high resolution X-ray images of these SNRs.

In the following sections of the paper we present the X-ray data on these remnants and the point sources which they contain. In addition we present optical data, both imaging and spectroscopic follow-up, which we used to identify the X-ray sources. Later we provide arguments supporting an association between the Be/X-ray stars and the SNRs.

2. 0101−72.4

2.1. Point Source

Figure 1a shows a portion of the RHRI field centered roughly on the optical position of 0101−72.4, after background subtraction and smoothing with a 4″ (standard deviation) gaussian. The background rate was estimated locally using an annular region 1′–2′ centered on the remnant, which yielded the value 2.0×10^{-6} counts s^{-1} arcsec^{-2}. The X-ray emission from 0101−72.4 is consistent with a point source at position (J2000) $1^h\ 3^m\ 12.6^s$, -72° 9′ 14.9″ (±2″, statistical error only). The source has a signal-to-noise ratio greater than 7 and a counting rate (corrected for dead-time, vignetting, quantum efficiency, and the counts scattered out of the standard detection cell) of $(4.90\pm0.70)\times10^{-3}$ s^{-1}. Assuming a power-law spectrum with a photon index between 1–2 and column density between 1.0×10^{21} cm^{-2} and 2.3×10^{21} cm^{-2} (see below), we infer a flux of $(1.6 \pm 0.2) \times 10^{-13}$ erg s^{-1} cm^{-2} in the 0.2–2 keV band. We searched for variability in the RHRI data down to timescales of roughly 1 s using a combination of Fourier Transforms and light curve folding, and not surprisingly, since we had only 88 source counts, found nothing significant.

This source also appears point-like in the ROSAT PSPC image. The background-subtracted PSPC counting rate (0.2–2.0 keV) is $(2.0 \pm 0.3) \times 10^{-3}$ s^{-1} for an exposure time of 3844 s (which is less than the nominal exposure time because we rejected data during time intervals with higher background rates, which occurred near the ends of the good time intervals supplied by the ROSAT standard processing). For the range of spectral parameters quoted above, the inferred flux is $(2.4 \pm 0.2) \times 10^{-13}$ erg s^{-1} cm^{-2}, some 50% higher than the RHRI flux. The spectral capability of the PSPC allowed us to constrain the column density to the source. At 90% confidence N_H must be greater than 7.7×10^{20} cm^{-2}, which clearly establishes that the source is in the SMC.

This region of the sky was imaged three times by the *Einstein Observatory*: twice with the IPC and once with the high resolution imager (EHRI). Seward & Mitchell (1981) quote an IPC count rate of 0.022 s^{-1} (for which we infer an error of 15%–20%) on 2 May 1979. Roughly six months later on 13 November 1979, the IPC rate was 0.0112 ± 0.0018 s^{-1} (Inoue, Koyama, & Tanaka 1983, Harris *et al.* 1993), about a factor of 2 less. On 18 April 1980, the EHRI provided a marginal detection at a count rate of $(1.8 \pm 0.5) \times 10^{-3}$ s^{-1}. The count rates from the latter two observations are consistent with the RHRI rate for the set of spectral parameters quoted above.

Narrow-band optical interference filter images of this SNR from an observing session on the 1.5-m telescope at CTIO on 22 November 1986 were used to identify the optical counterpart to the X-ray source. CCD images taken through a focal reducing camera (borrowed from R. Teske) in 5 different bands were available: Hβ, [O III] λ 5007, a continuum band centered on 6100 Å, Hα, and the [S II] doublet $\lambda\lambda$ 6716, 6731. The Hβ, [O III], and [S II] filters were all 50 Å wide (FWHM), the 6100 Å filter was 150 Å wide, and the Hα filter (in order to avoid [N II] λ 6583) was only 15 Å wide. Exposure

times were 1000 s for all but the continuum filter, for which a 300 s exposure was used. The images were bias-subtracted and flat-fielded using images of an uniformly illuminated screen within the dome. Observations of white dwarf standard stars (LTT 1020 and LTT 2415) were carried out at the beginning and end of the night in order to flux calibrate the SNR images. The conditions were not photometric on this night and the average residual error in flux calibration based on comparing the two standard stars was ~25%. Positions from the HST guide star catalogue were used to register our images to the sky. There were 11 catalogued stars within the roughly 10′ field, which provided an astrometric solution with an RMS position error of 0.3″. The plate scale was determined to be 0.83″ per pixel. In Figure 1b we show a portion of the Hα image at the same spatial scale and covering the same area of the sky as the X-ray image.

Low resolution spectra made from the filter-band imaging data are shown as the data points in Figure 2. The horizontal error bars denote the widths of the filters and the vertical ones show the flux calibration error. We show data for the two brightest stars within 15″ of the X-ray source position. The points near the middle of the plot are for the optical source which we identify as the X-ray emitter. This object, which is indicated on the Hα image, is at position $1^h\ 3^m\ 13.86^s$, $-72°\ 9'\ 14.1''$, approximately 5.9″ from the X-ray source position. Although this positional offset is larger than the quoted statistical error, ROSAT HRI positions are subject to systematic boresight corrections of 10″ or so, due to unknown time-varying errors in aspect reconstruction (David *et al.* 1992). The brighter stellar object 11.8″ south and 4.3″ west of the candidate is considerably redder: its filter-band data are shown at the top of Figure 2. These data are roughly consistent with a reddened ($A_V \sim 2.5$) star of spectral class F or G.

We obtained follow-up optical spectrophotometry of the blue candidate star during two separate runs with the CTIO 4m telescope and the RC spectrograph. The red portion of the spectrum (λ 5100 – 9600 Å) was observed on 1992 December 12 UT for a total of 900 sec at a resolution of 16 Å. The blue portion (λ 3200 – 7500 Å) was observed on 1992 December 18 UT for a total of 960 sec at a resolution of 9 Å.

Both of the nights were photometric, allowing us to obtain spectrophotometric data. Each observation of the star was performed through both a 3″ slit (matched to the resolution of the spectrograph) and a 10″ slit to ensure that we collected all of the light. Standard stars from Hamuy *et al.* (1992) were observed with a 10″ slit to provide flux calibration. The data were reduced using standard IRAF procedures. After flux calibration, the observations with the 3″ slit were corrected to the flux level of the 10″ slit. The resulting red and blue spectra showed an offset of approximately 2% in the absolute flux calibration. The blue spectrum was shifted up by this factor, and the two spectra were combined to form the spectrum shown as the curve in Figure 2. The agreement with the filter-band data is also excellent.

Synthetic photometry was performed on the resulting spectrum and we determined the following magnitudes: 14.73 (B), 14.80 (V), 14.74 (R), and 14.68 (I). The errors are

roughly ±0.05 magnitudes, including the 2% shift in the blue spectrum, which accounts for ~0.02 magnitudes of the total error.

The most striking feature of the spectrum in Figure 2 is the presence of strong Balmer line emission. Hα and Hβ are evidently in emission and there is some Hγ emission filling in the absorption feature. The remaining lines of the Balmer series are all seen in absorption. The equivalent width of Hα is the same for both the red and blue spectra (22 Å) and the filter-band data from several years earlier appear to show a comparable level of Hα emission. The Hβ equivalent width is 1.7 Å. The emission lines are unresolved at the resolution of our spectra. There are also several absorption features of which He I λ 4471 and λ 4025 are the strongest. While precise MK spectral typing requires higher resolution spectra than we have here, we estimate a spectral class around B0 based on the strength of He I λ 4471 relative to Mg II λ 4481, and the (possible) presence of He II λ 4686 (a significant flat-field correction to the spectrum near this line makes its identification less secure than we would like). The absence of Si III λ 4552 and Si IV λ 4089 argues against a supergiant classification. From the measured colors and assuming a spectral class O9 - B1 (V-III), we determine the reddening E(B–V) to be $0.23^{+0.01}_{-0.04}$ mag.

The mean wavelengths of the strongest spectral features for the star are all redshifted by a (heliocentric) radial velocity of ~175 km s^{-1}, which is consistent with the radial velocity of the SMC (168 km s^{-1}, Allen 1973). For a distance modulus to the cloud of 18.8 ± 0.1 (van den Bergh 1989), we derive an absolute V-magnitude range of −4.5 to −4.9, which is in excellent agreement with the spectral type estimated above. Based on the spectral type and the strength of the Balmer emission lines, we conclude that the optical source is a Be star in the SMC. Further support for this identification comes from the star's V−I color which is redder than a normal B star by about 0.2 magnitudes. This has been observed in other Be stars (*e.g.*, Bessel & Wood 1993) and has been interpreted as being due to the presence of additional light in the I passband from hydrogen recombination radiation. The inferred luminosity of the X-ray source (0.2–2 keV band) assuming it is in the SMC is 6.3×10^{34} erg s^{-1}, which is consistent with the level of persistent X-ray emission from other Be/X-ray star systems discovered by ROSAT (Motch *et al.* 1991) or known previously (White 1989).

2.2. Supernova Remnant

There is no obvious diffuse X-ray emission from either the shell or the interior of the SNR. The 3σ upper limit to the RHRI count rate limit from the region comprising the optically emitting SNR is 4.5×10^{-3} s^{-1}, excluding the counts from the point source. This implies an upper limit to the X-ray luminosity (0.2–2 keV band) of 7×10^{34} erg s^{-1} for an assumed temperature of 0.2 keV, abundance of 0.2 (relative to solar, see Russell & Dopita 1992) and column density of 1.6×10^{21} cm^2. We estimate the mean density of hot gas within the optical shell of the SNR to be $\lesssim 0.5$ cm^{-3}.

The filter-band data provide important additional information about the SNR. However discriminating between emission from stars and the diffuse nebula is difficult in such a crowded field. The four spectral line images were registered to the continuum frame using the positions of 10 isolated, bright (but unsaturated) stars. Then the continuum frame was smoothed slightly to reduce statistical fluctuations. Instead of subtracting this image from the others, which produced unsatisfactory results, we pursued the derivation of quantitative results using the following procedure. Counts in the spectral line images were masked-out (that is set equal to zero) based on the count value of the corresponding pixel in the smoothed continuum frame. We choose a conservative limit: all pixels with count values greater than 1σ above the sky in the continuum frame were masked-out. This removed a considerable fraction of each image; nevertheless there was still a large area of the SNR left. We selected several disjoint spatial regions which covered the bright rim of the SNR and extracted the counts from these regions for each masked-out image. For the sky the modal count value in each masked-out image was used.

We use the Hα to Hβ ratio to determine the reddening to the SNR. The mean value of the ratio is 3.73, while the variation in line ra- with position gives an uncertainty of $(-0.48, +0.34)$. Observational uncertainties due t- ounting statistics, errors in determining the sky value, the relative flux calibration, a-d emission from unresolved stars root-sum-square to a value of roughly 9%. The intrinsic ratio is 2.87 (Case B for $T_e = 10^4$ K) and varies less than $\sim$10% unless the temperature is much lower than expected for shock-heated gas (Osterbrock 1989). Using a standard reddening curve (*e.g.*, Zombeck 1990) we determine E(B–V) to be $0.23^{+0.08}_{-0.12}$. The equivalent hydrogen column density is estimated to be $(1.6^{+0.6}_{-0.8}) \times 10^{21}$ cm^{-2} (Gorenstein 1975). These are the values we used in estimating the X-ray fluxes above. The column density due to gas in the Galaxy is only about 3×10^{20} cm^{-2} in this direction (Seward & Mitchell 1981), so most of the absorption we see must be intrinsic to the SMC. The maximum absorption due to gas in the SMC is roughly 4×10^{21} cm^{-2} in this vicinity based on the 21 cm integrated brightness maps of Hindman (1967).

The positional variation of the Hα to Hβ ratio is apparently significant, and may indicate differential extinction across the face of the remnant. The sense of the variation is such that the western filament shows less absorption than the southern one. However, other line ratios that we can construct from our narrow-band images, *e.g.*, [S II]/Hα and [O III]/Hβ also appear to show a correlation with position. [O III]/Hβ is higher in the western filament compared to the southern one, while [S II]/Hα is higher in the southern filament.

Finally we point out a weak ring-like feature in the optical image of 0101−72.4 centered about 20″ southeast of the optical candidate to the X-ray source. The feature extends from a radius of about 15″ to 30″. It has an [O III]/Hβ ratio more than a factor of two greater than the average of the bright regions of the shell and [S II]/Hα is larger (by 50%) as well. From its appearance and the optical line ratios, we speculate that the ring may be

emission from SN ejecta. If so, the weakness of the optical emission and the lack of X-ray emission would indicate expansion into a low density medium, like the cavity formed by an earlier SN. A search for high velocity oxygen emission should be able to confirm or refute this speculation.

3. 0104−72.3

3.1. Point Source

Figure 3a shows a portion of the RHRI field approximately centered on the optical position of 0104−72.3, after background subtraction and smoothing with a 4″ (standard deviation) gaussian. As before, the background rate was estimated locally using an annular region 1′–2′ centered on the remnant, which yielded the value 1.8×10^{-6} counts s^{-1} arcsec^{-2}. The X-ray emission from 0104−72.3 consists of two parts: a diffuse component extending to the north and an unresolved source toward the south. Below we discuss the diffuse emission; here we focus on the point source at position (J2000) $1^h\ 6^m\ 18.0^s$, −72° 6′ 0.5″ (±2″, statistical error only). It was detected with a signal-to-noise ratio >5 at a counting rate (corrected in the same way as above) of $(3.1 \pm 0.5) \times 10^{-3}$ s^{-1}. Assuming a power-law spectrum with a photon index between 1–2 and column density between 4.0×10^{20} cm^{-2} and 1.2×10^{21} cm^{-2} (see below), we infer a flux of $(1.0 \pm 0.2) \times 10^{-13}$ erg s^{-1} cm^{-2} in the 0.2–2 keV band. For the ∼60 source counts we found no significant time variability down to timescales of roughly 1 s.

The ROSAT PSPC count rate from the entire source is $(3.1 \pm 0.4) \times 10^{-2}$ s^{-1} (0.2–2.0 keV). The two emission components were marginally resolved and roughly 30% of the counts came from the unresolved source toward the south. We estimate the point source flux to be $\sim 1 \times 10^{-13}$ erg s^{-1} cm^{-2} during the PSPC observation for the range of spectral parameters given above. This is consistent with the RHRI flux. Spectral analysis was carried out on the entire source region. A reasonably good fit was obtained for a thermal model with $kT \sim 0.6$ keV and $N_{\rm H} \gtrsim 1.5 \times 10^{21}$ cm^{-2}, although it is not clear how reliable the measured temperature is given that the spectrum contains emission from both X-ray emission regions. Nevertheless, the relatively high line-of-sight column density plus the lack of detected photons below ∼0.4 keV show that both sources are in the SMC.

This source was not detected in the Seward & Mitchell (1981) survey of the SMC and during the followup IPC observation (Inoue *et al.* 1983), it was far off-axis and the count rate was unreliable. The Einstein HRI upper limit (3σ) to the rate from the point source alone was 1.6×10^{-3} s^{-1}, which is consistent with the RHRI rate.

Once again our optical filter-band images were used to identify possible counterparts to the X-ray point source. SNR 0104−72.3 was observed at CTIO on 21 November 1986 during the same run and using the same instrumentation as for 0101−72.4, and we carried out the same analysis procedures on the data as described above. The conditions were nearly photometric on this night and the average residual error in flux calibration based on comparing the standard stars taken at the beginning and end of the night was $\lesssim 2\%$. We used a combination of positions from the HST guide star catalogue and published astrometry (Mathewson *et al.* 1984) to register our images to the sky. There were only 2 usable guide stars in the optical field, but their positions were consistent with the 4 stars from Mathewson *et al.* (1984). The RMS error on position was 0.5″ and the plate scale

was the same as before. In Figure 3b we show a portion of the Hα image at the same spatial scale and covering the same area of the sky as the X-ray image.

The stellar object nearest to the X-ray position is also the brightest star in our bluest frame (*i.e.*, Hβ) within 30″ of the X-ray position. We show the filter-band imaging data for this candidate as the points near the bottom of Figure 2. This object, which is indicated on the Hα image, is at position $1^h\ 6^m\ 18.62^s$, -72° 6′ 3.5″, approximately 4.2″ from the X-ray source position.

We were unable to obtain follow-up optical spectroscopy for this candidate during the last observing season at CTIO. Nevertheless we are confident that this source is also a Be star in the SMC. The filter-band data show strong Hα emission and a blue continuum. We point out that filter-band imaging using V, R, I, and a narrow Hα band has been used by others (Bessel & Wood 1993) to identify Be stars in the Magellanic Clouds. Indeed the similarity between these data and both the filter-band and spectral data from the Be star we identified above in 0101−72.4 is striking. We estimate the V-band magnitude to be 16.7, which suggests a range of absolute magnitudes of −2.2 to −2.9 assuming the SMC distance modulus and a reddening estimated at E(B–V) ∼ 0.05–0.25. This gives for the spectral type a range B2–B5 (luminosity class V–III). The X-ray flux implies a luminosity of 4.0×10^{34} erg s^{-1} (0.2–2 keV) for a source in the SMC, once again consistent with the level of persistent X-ray emission expected from Be stars.

3.2. Supernova Remnant

There clearly is diffuse X-ray emission from this remnant. The RHRI count rate within a 60″ radius circle centered on the optical emission, excluding the counts from the point source, is $(8.3 \pm 1.3) \times 10^{-3}$ s^{-1}. For a temperature of 0.2 keV, abundance 20% of solar. and a column density of 7×10^{20} atoms cm^{-2}, we infer a luminosity of 1.4×10^{35} erg s^{-1} (0.2–2 keV).

This remnant has been studied optically by Russell & Dopita (1990). The Hα to Hβ ratio we derive from the filter band data (3.99) is consistent within our systematic errors with the ratio they derived from spectroscopy. This line ratio varies hardly at all (∼ ± 2%) over the image of the remnant, suggesting spatially uniform extinction. To determine the reddening to the SNR, Russell & Dopita (1990) employed 2 techniques using several line ratios and obtained a value of $E(B-V) = 0.10^{+0.07}_{-0.05}$. Here we explicitly assume the minimum reddening to the SMC is 0.05 (Bessel 1991). This indicates a hydrogen column density along the line of sight of $(7^{+5}_{-3}) \times 10^{20}$ atoms cm^{-2}.

In the radio band, albeit with poorer angular resolution, this remnant reveals a double lobe shape similar to the optical, although the radio flux density is considerably less than that from similar sized SNRs in the LMC. The lack of X-ray emission from the optically bright lobes implies an upper limit on the density of hot ($kT \sim 0.2$ keV) gas of roughly

0.5 cm^{-3}. The diffuse X-ray emission comes from a region without obvious optical emission. This may merely be highlighting a region of higher temperature, which has not yet developed a fully radiative shock, as elsewhere in the remnant.

4. DISCUSSION

Be stars in the SMC are the most likely identifications for the point-like X-ray sources seen in these two SNRs. The observed X-ray luminosities are consistent with this interpretation, while other classes of X-ray emitting sources in the SMC, such as normal stars or CVs, would fail to produce the observed flux by at least a factor of 100. We can eliminate a random extragalactic source since the probability of finding such a source at the appropriate flux level within a 1′ radius circle (roughly the size of each SNR) is $\lesssim 0.4\%$, extrapolating from the *Einstein* medium sensitivity survey (EMSS, Gioia *et al.* 1990). Galactic stars are also unlikely identifications, since any reasonable candidate would need to be no brighter than $V \sim 18$ (based on our optical imaging data) and this would require an X-ray to optical flux ratio larger than the vast majority of stars identified in the EMSS sample. In addition, the intrinsic X-ray absorption to these sources, as determined by the PSPC spectral data, militates against a Galactic origin and is consistent with the sources being in the SMC. Time variability in the X-ray flux, as observed for the source in 0101−72.4, which is a common characteristic of Be/X-ray stars, provides additional evidence in support of the identification. Lastly we can improve the positional agreement between the Be stars and X-ray sources by applying a simple boresight correction to the X-ray data. If we shift the X-ray derived positions to the west by 4.4″ and to the south by 1.1″, then the difference in the X-ray and optical positions is reduced to 2.4″ for both sources, which is within the statistical uncertainty. This boresight correction is well within the level expected given the current accuracy of ROSAT image reconstruction.

How likely is it that the Be/X-ray stars are associated with the SNRs? The agreement in inferred optical extinction values suggests a physical, rather than merely a projected, association. Be/X-ray binary star systems with X-ray luminosities at least as large as we observe here ($\sim 5 \times 10^{34}$ erg s^{-1}) occur roughly once every 1000 or so B stars based on observational evidence (Grillo *et al.* 1992; Meurs *et al.* 1992) as well as theoretical arguments (Pols *et al.* 1991). Within the areas (~3 square arcmin) of 0101−72.4 and 0104−72.3 there are 79 and 68 stars, respectively, down to $V \sim 19.5$, which should be complete for B stars in the SMC, assuming negligible extinction. We estimate that roughly 20% of these are B stars using data on galactic stars from Allen (1973) (most are K giants). This gives a chance probability for each association of about 1.5%. Further support for a low probability comes from the following argument. If the areas of the sky near the SNRs were typical and the occurrence of Be/X-ray stars were proportional to the projected density of stars, then we should expect to see, within each optical image, roughly 35 other Be/X-ray star systems similar to the two we have discovered, since the density of stars is not obviously greater near the SNRs than elsewhere in these fields. We see no other point sources in the optical fields with X-ray fluxes within a factor of ~3 of the two we have discovered, which suggests that the objects found in the SNRs are atypical.

On the other hand, it seems unlikely that the same SN explosions which gave rise to the remnants also formed the neutron stars in the Be/X-ray binaries. From the present

positions of the Be/X-ray stars and making estimates of the remnants' ages and the sites of the explosions, we can derive values for the transverse speeds of the star systems. We estimate a value of $v = 570\,(t_4/1.5)^{-1}$ km s^{-1} for 0101−72.4 and $v = 500\,(t_4/1.5)^{-1}$ km s^{-1} for 0104−72.3, where t_4 is the age of the remnant in units of 10^4 yr. The age we have used corresponds roughly to the onset of the radiative phase of evolution for a remnant of size 25 pc and for metallicity appropriate to gas in the SMC. It might be possible that the remnants are older by a factor of 2 or maybe even 3. The site of the explosion is also rather uncertain, but even when the maximum reasonable uncertainty for this is combined with an increased age, the minimum transverse speed would still be of the order of 100 km s^{-1}, certainly large for a high-mass X-ray binary (van Oijen 1989). Our data do not indicate a large radial velocity for the source in 0101−72.4, however this does not conclusively refute the hypothesis.

An alternate, and perhaps more palatable, explanation for the apparent association is that the precursor to the SNR and the Be/X-ray binary were common members of an OB association in the SMC. This would provide a physical association, but would not demand a direct relationship. If we reconsider the possibility for a chance association, but now assume that all of the observed stars near 0101−72.4 and 0104−72.3 are spectral type B, then the probability that either association is random (based on the number of stars present now) increases from 1.5% to a more likely value of about 7.5%. However, the joint probability that *both* associations have arisen by chance in this manner is still uncomfortably small. Furthermore, this hypothesis requires that there had been two SNe in the relatively recent past in the vicinity of each SNR (one to make the remnant and the other to make the neutron star in the binary). The Be star in 0101−72.4 should have a lifetime of about 10^7 yr. Thus the putative OB associations must be rich enough to have produced two SNe in the last few million years and the turnoff masses of the clusters should be consistent with the observed spectral types of the Be stars we have discovered.

Hodge (1985) has cataloged OB associations in the SMC. Nos. 54 and 57 in his list are the associations nearest to these SNRs; the former is some 3′ away from 0101−72.4, while the latter is more than 7′ away from 0104−72.3 (based on Hodge's cataloged positions). Both of these associations are easily visible on our optical images (although they are outside the regions shown in Figures 1b and 3b) but it is also clear that their apparent boundaries are several arcminutes away from the SNRs.

We are aware of at least one other case of a chance association between a SNR and a Be/X-ray star. In a recent article Gorenstein, Hughes, & Tucker (1994), in addition to discovering soft X-ray emission from SN1987A, present evidence for the existence of a Be/X-ray binary only 30″ from the site of the SN explosion in a region known to coincide with a B association in the LMC. An optical counterpart was not directly identified, but several plausible candidates were suggested. It is quite possible that there are other examples of associations between Be/X-ray stars and SNRs in the LMC, although none have been reported, since the fields of these SNRs have not been sufficiently explored.

There are eight catalogued LMC SNRs with diameters between 20 and 35 pc. Three of these are very bright (N132D, DEM71, and N49B) with X-ray luminosities 2 orders of magnitude more than our Be stars and hence given the distance to the LMC and the limited spatial resolution of current X-ray telescopes, we would not expect to be able to see X-ray point sources of the appropriate luminosity. For two of the remnants there is no information available on X-ray structure at arcsecond scales. The remaining three remnants all show evidence (based on *Einstein* HRI data) for clumpy or patchy X-ray emission, which could easily hide a weak point source. To our knowledge, no one has attempted to identify plausible X-ray sources with optical counterparts in these SNRs.

5. CONCLUSIONS

We have obtained the first high resolution X-ray images of two SNRs in the SMC, 0101−72.4 and 0104−72.3. These images reveal the presence within the optical boundaries of the SNRs of unresolved X-ray sources with luminosities (0.2–2 keV) of $\sim 5 \times 10^{34}$ erg s^{-1}. We identify these with Be stars in the SMC. Since the Be/X-ray stars are not near the centers of the remnants, a direct association between them would require rather large space velocities ($\gtrsim$ 100 km s^{-1}) for the binaries. Alternatively, the associations between the SNRs and Be/X-ray stars could be the result of common membership in OB associations in the SMC. The probability that the SNRs and Be/X-ray stars are unrelated, and that the association is merely random, is small: $\lesssim 1.5\%$ in each case.

Given the likelihood that these SNRs are associated with a Population I environment, we draw the conclusion that they are most probably the remnants of massive-star (*i.e.*, Type II) SN explosions. In this situation 0104−72.3 would not be a Balmer-dominated remnant as suggested by Mathewson *et al.* (1984) since that is believed to be strongly indicative of a Type Ia SN origin, as in the Galactic remnants of SN 1572 (Tycho) and SN 1006. The diffuse X-ray emission from the two SMC remnants is weak ($<7 \times 10^{34}$ erg s^{-1} for 0101−72.4 and 1.4×10^{35} erg s^{-1} for 0104−72.3), but we believe that is largely due to the low metallicity of the SMC. Most of the X-ray flux from a plasma at a temperature of 0.2 keV comes from line emission and so the intrinsic emissivity varies very nearly in direct proportion to the metal abundance. The intrinsic emissivity of gas in the SMC (with mean abundance 0.2 of solar) is a factor of 4.5 less than the intrinsic emissivity of gas with solar abundances. Although this makes detailed study of the SMC remnants in the X-ray band difficult, there are still valuable lessons which can be learned from such observations, as we have shown in this article.

ACKNOWLEDGEMENTS

J. P. H. thanks K. Koyama for providing a hospitable environment during his visit to Kyoto University where this paper was written. He also thanks R. Kirshner and P. F. Winkler for their able training in optical observation techniques. Dick Teske lent us his focal reducing camera for the imaging run and we acknowledge his contribution. We thank M. Phillips for taking the red and blue spectra of 0101−72.4 for us. Conversations with R. Brissenden, P. Massey, J. McClintock, N. Suntzeff, and A. Walker were productive and helpful. We appreciate the comments that M. Birkinshaw, D. Helfand, and H. Tananbaum made on this manuscript. This research was supported in part by NSF Grant No. INT-9308299, NASA Grants NAG5-1724 and NAG5-2156, and Smithsonian Institution funds.

REFERENCES

Allen, C. W. 1973, Astrophysical Quantities, 3rd ed., (London: The Athlone Press)

Aschenbach, B. 1988, Appl. Optics, 27, 1404

Bessel, M. S. 1991, A&A, 242, L17

Bessel, M. S., & Wood, P. R. 1993, in New Aspects of Magellanic Cloud Research, ed. B. Baschek et al. (Berlin: Springer-Verlag), 271

David, L. P., Harnden, F. R., Jr., Kearns, K. E., & Zombeck, M, V, 1992, The ROSAT High Resolution Imager, U.S. ROSAT Science Data Center report, p. 4

Gorenstein, P. 1975, ApJ, 198, 95

Gorenstein, P., Hughes, J. P, & Tucker, W. H. 1994, ApJ, to appear 1 Jan

Grillo, F., Sciortino, S., Micela, G., Vaiana, G., & Harnden, F. R., Jr. 1992, ApJS, 81, 795

Hamuy, M., Walker, A. R., Suntzeff, N. B., Gigoux, P., Heathcote, S. R., & Phillips, M. M. 1992, PASP, 104, 533

Harris, D., *et al.* 1993, The *Einstein* Catalogue of IPC X-Ray Sources, NASA Technical Memorandum 108401, p. 28

Hindman, J. V. 1967, Australian J. Phys., 20, 147

Hodge, P. 1985, PASP, 97, 530

Hughes, J. P. 1994, in preparation

Inoue, H., Koyama, K., & Tanaka, Y. 1983, in IAU Symposium 101, Supernova Remnants and their X-Ray Emission, eds., J. Danziger & P. Gorenstein (Dordrecht: Reidel), p. 535

Lang, K. R. 1992, Astrophysical Data: Planets and Stars (Berlin: Springer-Verlag), 722

Mathewson, D. S., Ford, V. L., Dopita, M. A., Tuohy, I. R., Long, K. S., & Helfand, D. J. 1983, ApJS, 51, 345

Mathewson, D. S., Ford, V. L., Dopita, M. A., Tuohy, I. R., Mills, B. Y., & Turtle, A. J. 1984, ApJS, 55, 189

Meurs, E., *et al.* 1992, A&A, 265, L41

Motch, C., *et al.* 1991, A&A, 246, L24

Osterbrock, D. E. 1989, Astrophysics of Gaseous Nebulae and Active Galactic Nuclei (Mill Valley: University Science Books), p. 80

Pfeffermann, E., *et al.* 1986, Proc. SPIE Int. Opt. Eng., 733, 519

Pols, O. R., Cote, J., Waters, L., & Heise, J. 1991, A&A, 241, 419

Russell, S. C., & Dopita, M. A. 1990, ApJS, 74, 93

Russell, S. C., & Dopita, M. A. 1992, ApJ, 384, 808

Seward, F. D., & Mitchell, M. 1981, ApJ, 243, 736

Trümper, J. 1983, Adv. Space Res., 2, 241

van den Bergh, S. 1989, A&AR, 1, 111

van Oijen, J. G. J. 1989, A&A, 217, 115

White, N. E. 1989, A&AR, 1, 85

Zombeck, M. 1990, Handbook of Space Astronomy and Astrophysics, 2nd. edition, (Cambridge: Cambridge University Press), p. 104

Zombeck, M. V., Conroy, M., Harnden, F. R., Jr., & Roy, A. 1990, in EUV, X-Ray, and Gamma-ray Instrumentation for Astronomy, SPIE Proc. Vol. 1344, eds.. O. H. W. Siegmund & H. S. Hudson, p. 267

FIGURE CAPTIONS

Fig. 1a – ROSAT HRI X-ray map of 0101−72.4. The contour levels start at a value of 2.34×10^{-6} counts s^{-1} arcsec^{-2} (3σ above background) and increase by multiplicative factors of 1.6. The crosses mark the positions of stars used for registering to the optical images.

Fig. 1b – Hα image of 0101−72.4 shown at the same scale as Fig. 1a. The optical candidate to the X-ray point source is indicated by the arrow. Note the weak ring-like diffuse feature centered about 20″ southeast of the optical candidate to the X-ray source. This feature shows stronger [O III] and [S II] emission (relative to Hα) than the main bright portions of the shell and we suggest that it might due to emission from SN ejecta (see text).

Fig. 2 – Optical spectral data of counterparts to the X-ray sources. The data points with error bars come from the filter-band images. The vertical error bars show the uncertainty in photometric calibration, while the horizontal error bars denote the widths of the several filters. The points at the top come from the brightest stellar object within 15″ of the X-ray source position in 0101−72.4, while the points in the middle come from the Be star which we propose as the counterpart. The points near the bottom of the figure are for the proposed counterpart to the X-ray source in 0104−72.3. A portion of the optical spectrum from the CTIO 4-m for the Be star in 0101−72.4 is also shown. The spectral resolution varies from 9 Å in the blue to 16 Å in the red. Hα and Hβ are evident in emission.

Fig. 3a – ROSAT HRI X-ray map of 0104−72.3. The contour levels start at a value of 1.98×10^{-6} counts s^{-1} arcsec^{-2} (3σ above background) and increase by multiplicative factors of 1.3. The crosses mark the positions of stars used for registering to the optical images.

Fig. 3b – Hα image of 0104−72.3 shown at the same scale as Fig. 3a. The optical candidate to the X-ray point source is indicated by the arrow.

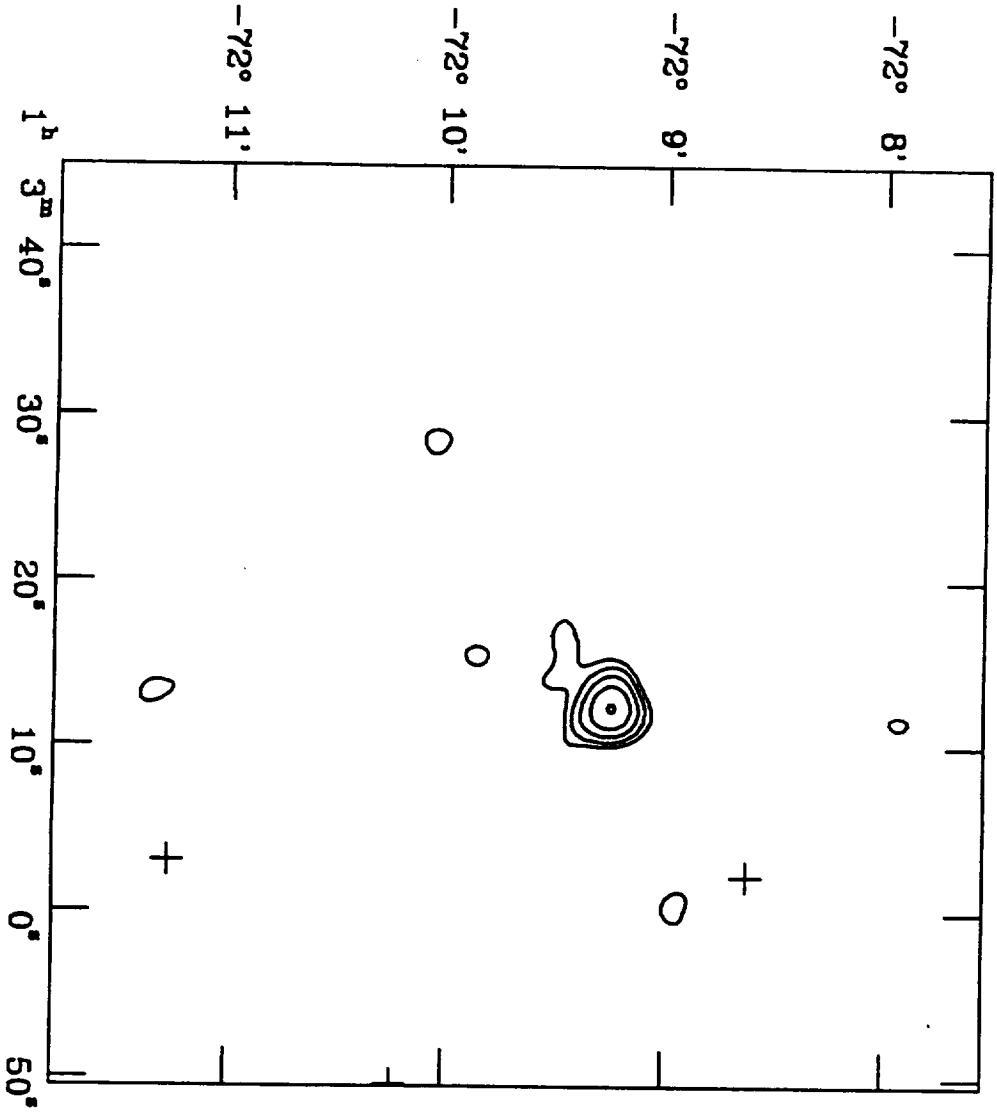

Figure 1a

NORTH

EAST

Figure 1b

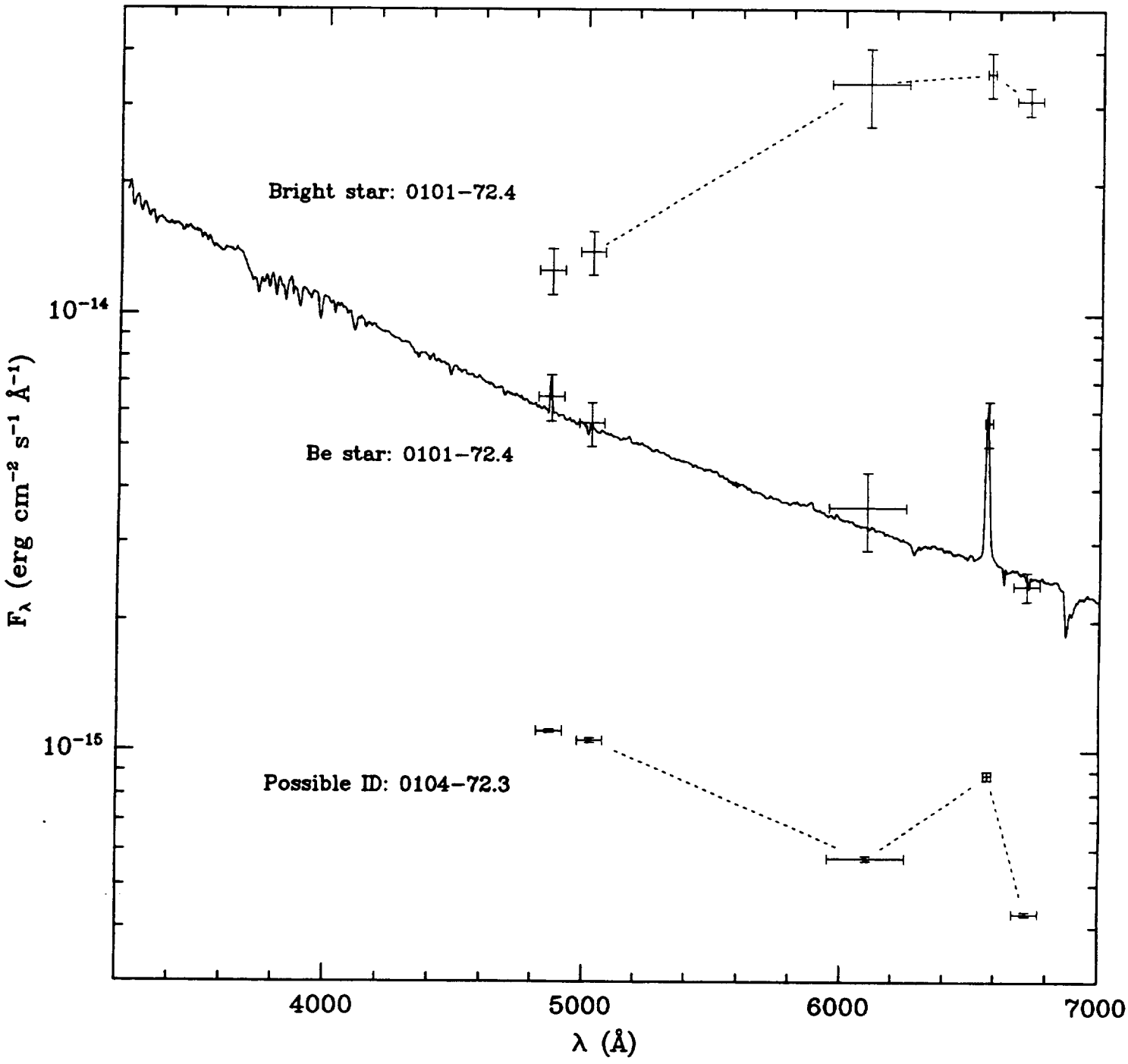
Bright star: 0101−72.4
Be star: 0101−72.4
Possible ID: 0104−72.3
10^{-14}
10^{-15}
F_λ (erg cm^{-2} s^{-1} Å^{-1})
4000
5000
6000
7000
λ (Å)

Figure 2

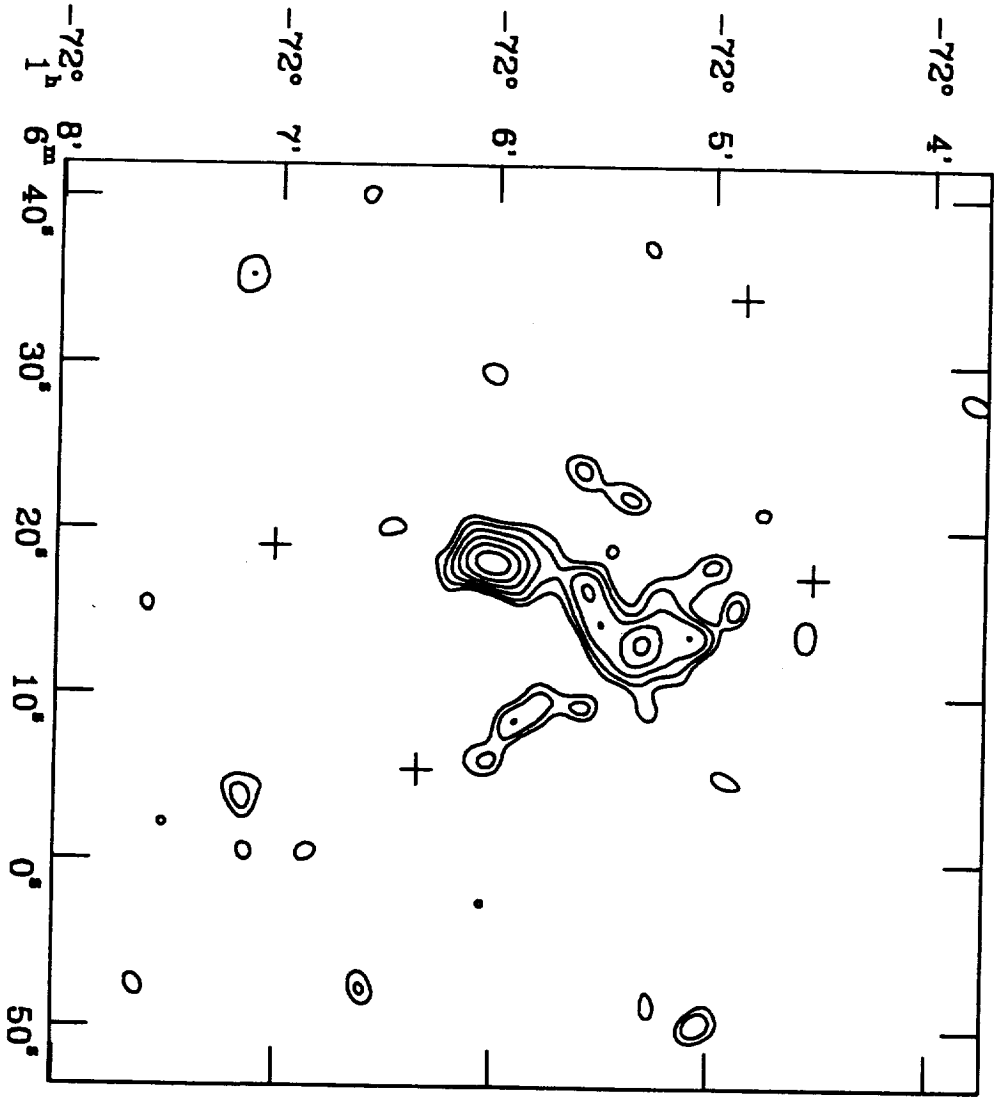

Figure 3a

NORTH

EAST

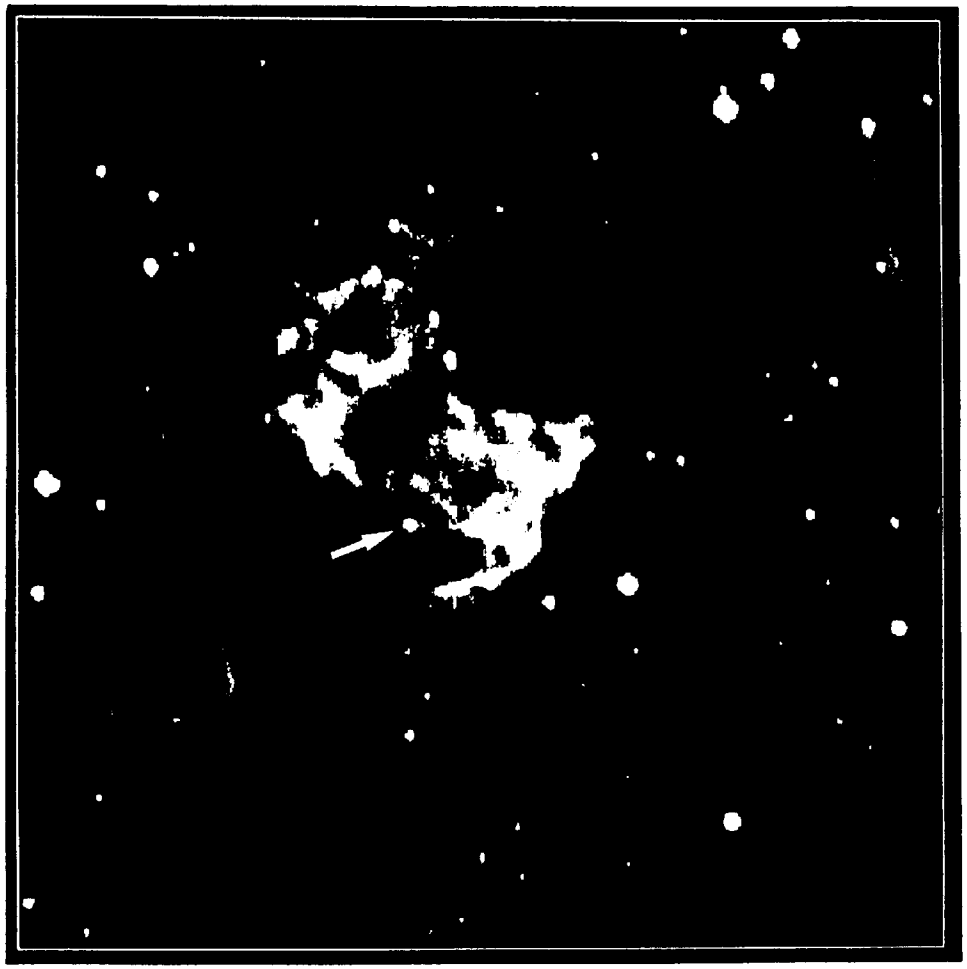

Figure 3b

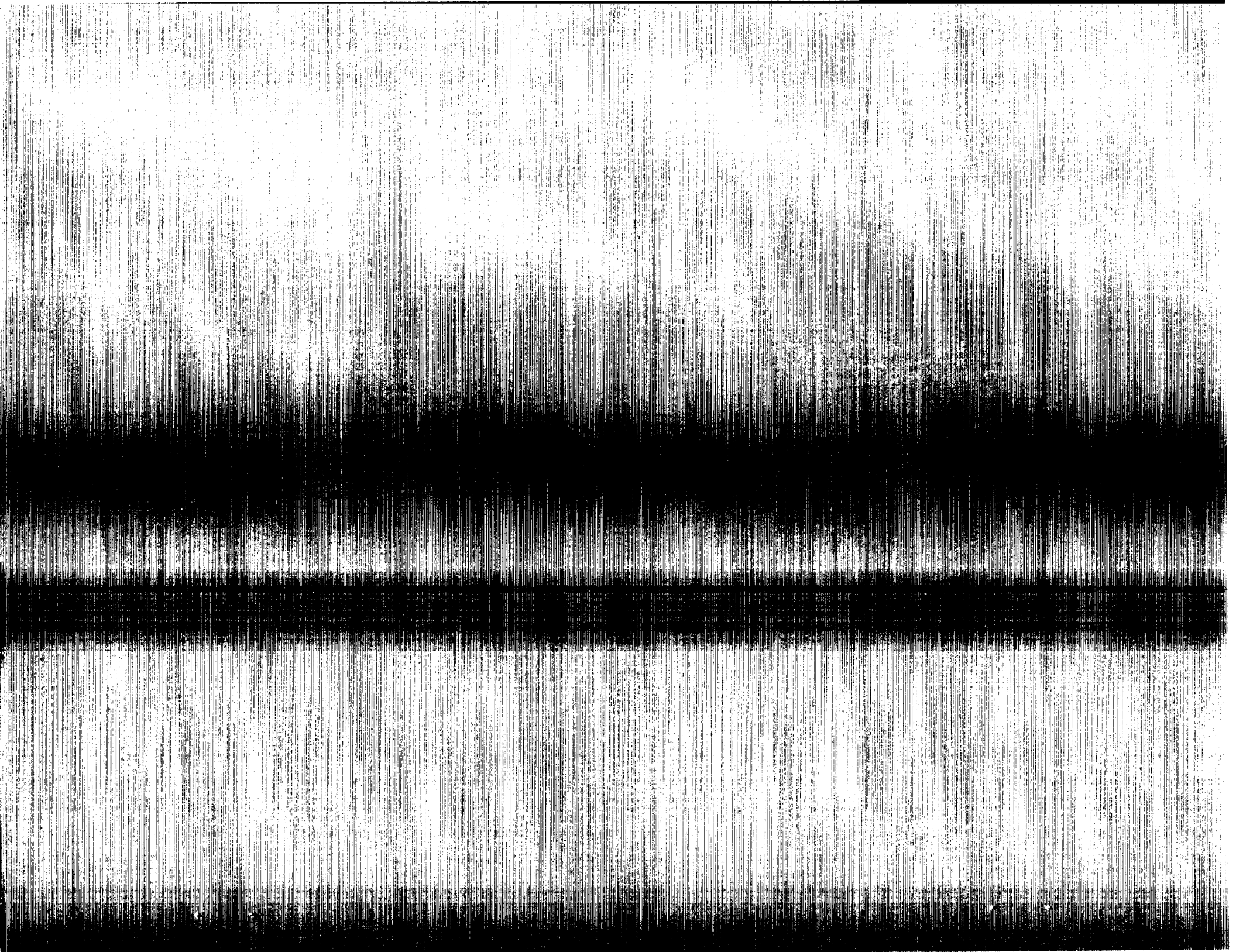

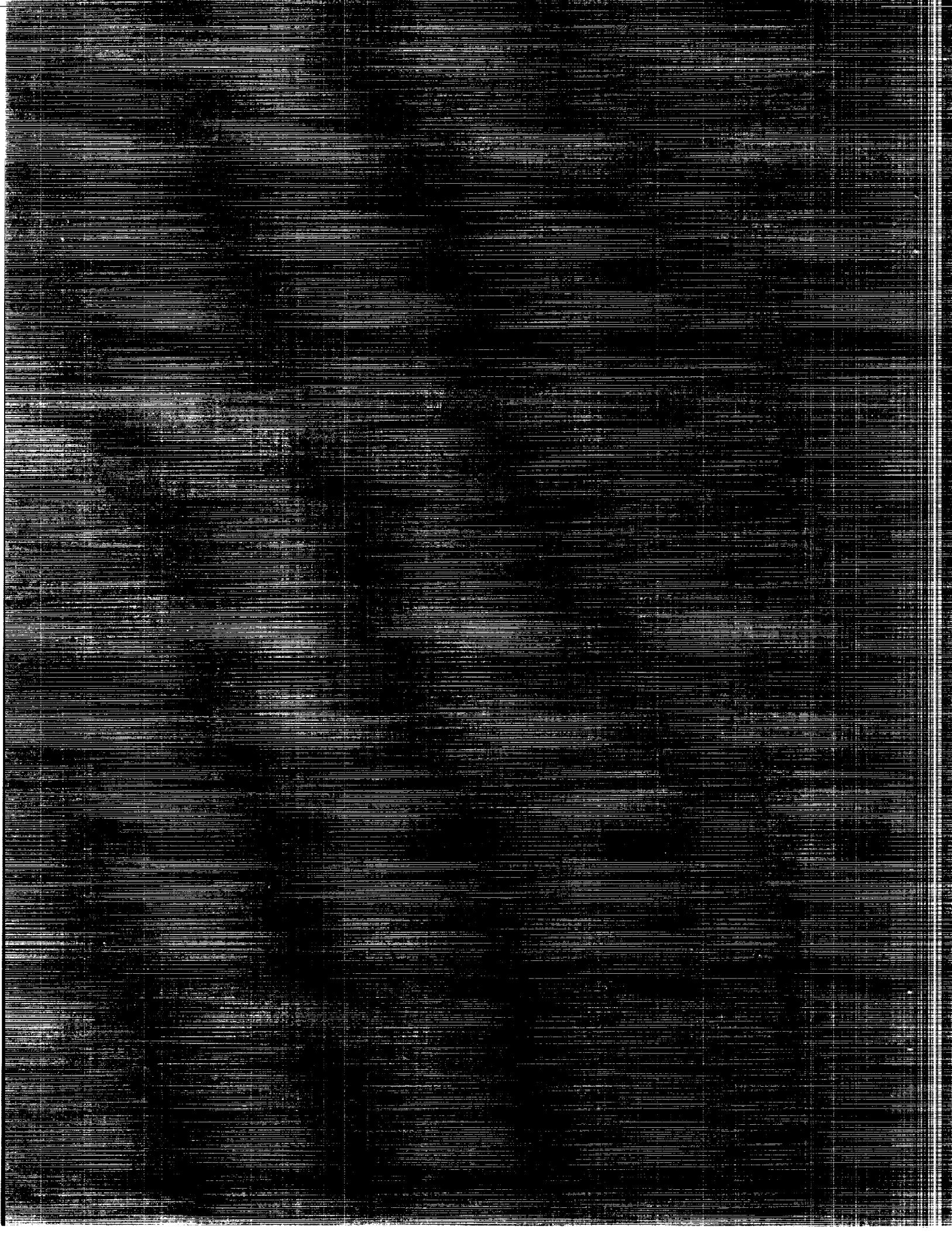

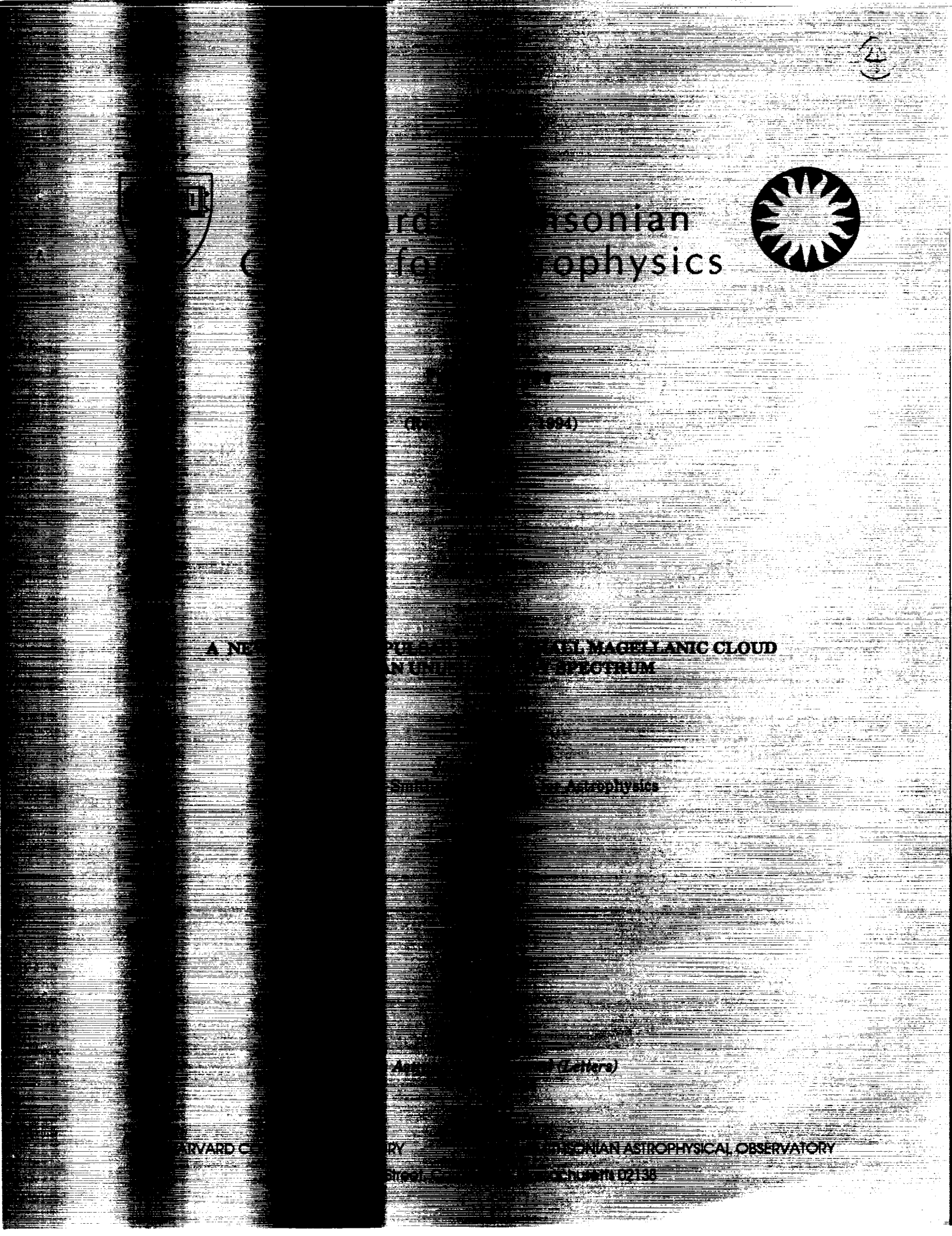

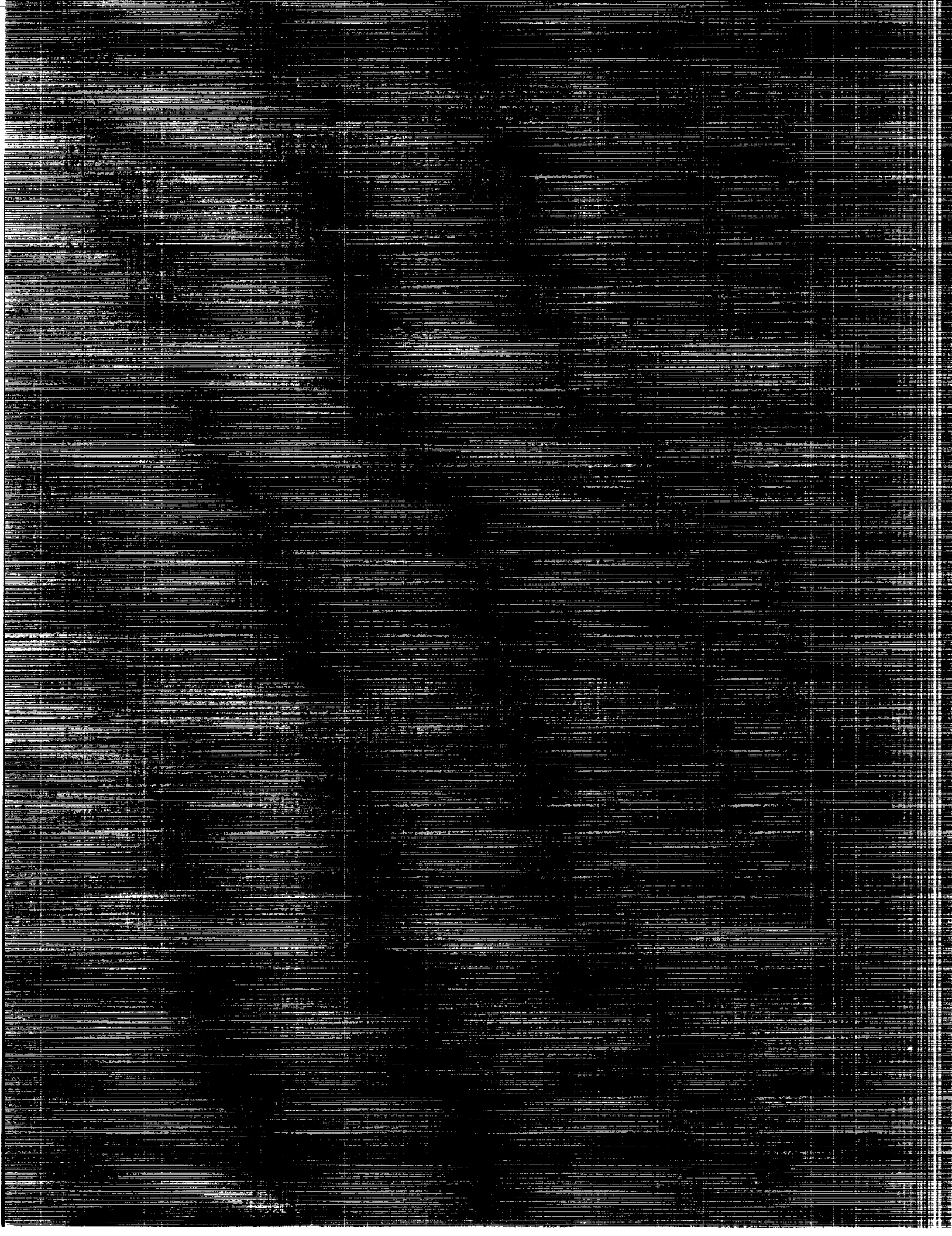

Center for Astrophysics
Preprint Series No. 3839

A NEW TRANSIENT PULSAR IN THE SMALL MAGELLANIC CLOUD WITH AN UNUSUAL X-RAY SPECTRUM

John P. Hughes[1]
Harvard-Smithsonian Center for Astrophysics
60 Garden Street, Cambridge, MA 02138

To appear in *The Astrophysical Journal Letters*, **427**, L25
May 20, 1994

Received: 2 February 1994
Accepted: 2 March 1994

Subject headings: binaries: general – pulsars: individual (RX J0059.2−7138) – stars: emission-line, Be – stars: neutron – X-rays: stars

[1] E-mail: jph@cfa.harvard.edu

ABSTRACT

This article reports the discovery of a luminous (3.5×10^{37} ergs s^{-1} over the 0.2–2 keV band) transient X-ray pulsar in the Small Magellanic Cloud (SMC) with an extremely soft component to its X-ray spectrum. This is the first time that a spectrum of this type has been seen in this class of X-ray source. The pulse period is 2.7632 s and the pulse modulation appears to vary with energy from nearly unpulsed in the low-energy band of the *ROSAT* PSPC (0.07–0.4 keV) to about 50% in the high-energy band (1.0–2.4 keV). The object, RX J0059.2−7138, also shows flickering variability in its X-ray emission on timescales of 50–100 s. The pulse-phase-averaged PSPC X-ray spectrum can be well described by a two component source model seen through an absorbing column density of $\sim 10^{21}$ atoms cm^{-2}. One spectral component is a power law with photon index 2.4. The other component is significantly softer and can be described by either a steeply falling power law or a blackbody with a temperature $kT_{BB} \sim 35$ eV. This component is transient, but evidently unpulsed, and, for the blackbody model fits, requires a large bolometric luminosity: near, or even several times greater than, the Eddington luminosity for a 1.4 $M_{\odot}$ object. When these characteristics of its soft emission are considered, RX J0059.2−7138 appears quite similar to other X-ray sources in the Magellanic Clouds, such as CAL 83, CAL 87, and RX J0527.8−6954, which show only extreme ultrasoft (EUS) X-ray spectra. The discovery of RX J0059.2−7138, a probable high-mass X-ray binary, clearly indicates that EUS spectra may arise from accretion-powered neutron-star X-ray sources. This result lends support to the idea that some of the "pure" EUS sources may be shrouded low-mass X-ray binaries rather than accreting white dwarfs.

1. INTRODUCTION

A possible new class of celestial X-ray sources, characterized by soft blackbody X-ray emission with temperatures in the range 30–100 eV, has recently been recognized based on observations by the *Einstein Observatory* (Long, Helfand, and Grabelsky 1981; Wang et al. 1991; Wang & Wu 1992) and *ROSAT* (Trümper et al. 1991; Greiner, Hasinger, & Kahabka 1991; Kahabka & Pietsch 1993; Pietsch & Kahabka 1993; Cowley et al. 1993; Schaeidt, Hasinger, & Trümper 1993; Orio & Ögelman 1993). In the several cases known, there is no measurable X-ray flux above 0.5 keV and so these objects have been referred to as supersoft or, in the nomenclature I will use, extreme ultrasoft (EUS) sources. Several models have been proposed to explain the high luminosities and soft spectra seen from these objects: scattering in an extended accretion disk corona (Fabian, Guilbert, & Callanan 1987), Compton scattering in an optically-thick cocoon surrounding a compact object undergoing supercritical accretion (Greiner et al. 1991), or the steady thermonuclear burning of hydrogen on an accreting white dwarf (van den Heuvel et al. 1992). In this article I report the discovery by *ROSAT* of a luminous, transient X-ray pulsar in the Small Magellanic Cloud (SMC) which clearly shows, in addition to the power-law spectral component which is typical for these sources, an EUS spectral component. A combination spectrum of this type is reminiscent of that observed from the Galactic X-ray binary pulsar Her X-1 during its high state. The presence of pulsars, i.e., rapidly rotating neutron stars, in the latter two sources argues convincingly against the accreting white dwarf model as the explanation for their EUS emission.

2. ANALYSIS

RX J0059.2−7138 appeared as a serendipitous source in a short pointing (4900 s) of the bright supernova remnant 0102−72.2 in the SMC carried out on 1993 May 12 with the *ROSAT* positional sensitive proportional counter (PSPC). It was some 33′ off-axis and had an exposure-corrected counting rate of 7.826 ± 0.047 s^{-1}. The best estimate of its position is $00^h59^m12.9^s$, $-71°38'50''$ (J2000), after accounting for (1) a translational shift of 6.4″ using the optical positions of two known sources near the center of the field; (2) a shift of 6.9″ to correct for the recently discovered roll angle error in the *ROSAT* standard processing; and (3) a shift of 7.4″ to compensate for the asymmetric shape of the coma-distorted image, due to the large field angle. This latter effect was "calibrated" using off-axis observations of LMC X-1 in other PSPC fields and it was verified by applying the technique to another source in the 0102−72.2 field (see below). The positional uncertainty is limited by these systematic effects and is estimated to be no more than about 10″ in each coordinate. Within the X-ray source error circle there is a $B_J \sim 14.1$ mag HST guide star at position $00^h59^m12.74^s$, $-71°38'44.7''$ (J2000), only 6″ from the X-ray position. Comparison of the B- and V-band images in the Hodge and Wright (1977) atlas of the SMC suggests that this star is bluer than its neighbors. The atlas also reveals another star fainter by about 1 magnitude approximately 11″ northwest of the HST guide star and about 16″ from the X-ray position. Any other plausible optical candidates within 20″ of the X-ray position must be significantly fainter ($m_V \gtrsim 16$) than these two.

The *ROSAT* standard processing detected this source and indicated the presence of variability on a timescale of about 2.7 s. Using standard IRAF/PROS tasks I confirmed this periodicity and refined the value of the pulse period (using period folding techniques and including barycenter corrections) to be 2.7632 ± 0.0002 s. Of the 32 known X-ray pulsars, only three have periods shorter than this value (White, Nagase, & Parmar 1994). The pulse profile is shown in Figure 1 in three separate energy bands (2 cycles are shown). One single broad pulse is seen. The pulse modulation (defined as maximum minus minimum divided by the average) apparently increases with energy: 0.13 ± 0.15 over the 0.07–0.40 keV band, 0.27 ± 0.20 over 0.40–1.0 keV, and 0.52 ± 0.17 over 1.0–2.4 keV.

The observation consisted of four nearly equal time intervals, nearly equally spaced over a period of 18,438 s. I determined the pulse period independently for each of the four data intervals and obtained values which were consistent with the period derived from the entire data set. The source count rates, averaged over each of these four intervals, were constant within the errors, varying by less than ±3% from the mean. On shorter timescales (50–100 s), however, RX J0059.2−7138 showed variability with excursions from the mean rate up to ∼30%. Because of the large image size (FWHM ∼1.5′), the wobble motion is not expected to introduce such a large modulation, and a direct comparison reveals that the wobble motion (at a period of 400 s) and the source variability were indeed uncorrelated. The variation in the soft (0.07–0.40 keV) and hard (0.40–2.40 keV) bands was weakly correlated (linear correlation coefficient ~ 0.2), but a definitive conclusion on this correlation is limited by the statistical error.

Examined over longer timescales, years to decades, the source is transient. It was not detected by *SAS* 3, which discovered SMC X-2 and SMC X-3 (Clark et al. 1978). It did

not appear in three separate pointings with the *Einstein Observatory* in 1979 and 1980, and *EXOSAT* failed to detect it in 1983 (Jones et al. 1985). As for previous observations with the *ROSAT* PSPC: the all sky survey (Kahabka & Pietsch 1993) in 1990 November and pointed observations (Pietsch & Kahabka 1993) in 1991 November, also showed no evidence for a source this bright at the appropriate position. The 3 σ upper limit to the flux (0.2–2 keV band) of the new source (assuming the same intrinsic spectrum as used below) was 1.5×10^{-13} ergs s^{-1} cm^{-2} on 1979 November 13 based on *Einstein* imaging proportional counter (IPC) data. On 1980 December 26 the upper limit was 5.3×10^{-14} ergs s^{-1} cm^{-2} based on data from the *Einstein* high-resolution imager (HRI). This is over a factor of 1500 less than the flux quoted here.

Below a cut-off energy of roughly 10–20 keV, X-ray pulsars tend to show power-law spectra (White et al. 1994) with photon indices $\alpha_P \sim 1.0$–2.0. The pulse-phase-averaged soft X-ray spectrum of RX J0059.2−7138 is not well described by such a single power law observed through a line-of-sight absorbing column with solar abundances (using the photoelectric absorption cross sections from Balucinska-Church & McCammon 1992, including more recent updates to the cross sections of helium). The minimum χ^2 for this model is 46.57 for 24 degrees of freedom (including in each channel a 1% systematic error added in quadrature with the statistical error), which can be rejected at the 99.6% confidence level. The residuals from this fit are at the level of 15%–20%, significantly more than the calibration uncertainties in the PSPC spectral response function. Other simple, single-component models, such as blackbody, exponential, or thermal plasma emission (Raymond & Smith 1977), also can be rejected with high confidence. Reducing the metal abundance of the absorbing material in the line-of-sight (as might be indicated by the lower metallicity of the SMC) does not yield a better fit. I obtain an acceptable fit (reduced $\chi^2 \sim 1.03$ for 22 degrees of freedom) with a two-component model, either two power-law models or a power law and blackbody, provided that the second component is quite soft. This represents a highly significant reduction in χ^2 ($\gg$ 99.95% confidence level) for introducing two additional free parameters. Results of spectral fitting with a power-law plus blackbody model are given in Table 1, and the data and model are plotted in Figure 2.

The best-fit column density for RX J0059.2−7138 is greater than the Galactic column in this direction [(3–7) $\times 10^{20}$ cm^{-2}], but it is also less than the total integrated column through this part of the SMC ($\sim 4 \times 10^{21}$ cm^{-2}, Hindman 1967). This result holds true even when different spectral models for the X-ray emission are used. This confidently places RX J0059.2−7138 within the SMC and also demonstrates that it is not self-absorbed by a thick overlying corona. The flux in the 0.2–2 keV band is 8.7×10^{-11} ergs s^{-1} cm^{-2}, which implies a luminosity of 3.5×10^{37} ergs s^{-1} for a distance of 57.5 kpc (van den Bergh 1989).

As Table 1 indicates, the bolometric luminosity of the blackbody component itself is quite large. However most of the luminosity from this component lies outside the *ROSAT* band; specifically, only some 15% of L_{BB} is above 0.2 keV, assuming the best-fit parameters in Table 1. In addition, the precise value of the blackbody component's luminosity is sensitive to the assumed shape of the higher energy spectral component. For example,

substituting an exponential for the higher energy component resulted in a reduction of a factor of 8 in L_{BB}, albeit with an increase in the best-fit χ^2 of 10.7 over the power-law plus blackbody model.

The results on the EUS spectral component are also sensitive to the X-ray absorption model used. When the data are fitted with Morrison & McCammon (1983) absorption cross sections and abundances, the derived luminosity of the blackbody component becomes about a factor of 2 larger than shown in Table 1. A more appropriate absorption model should consider the lower mean metal abundance of the SMC. If I assume that only part of the X-ray absorption (specifically, 3×10^{20} atoms cm^{-2}) comes from gas with solar composition while the remainder comes from gas with metallicity appropriate to the SMC (roughly 25% solar: see Russell & Dopita 1992), then the fits yield a luminosity of the blackbody component which is some 15% larger than that shown in Table 1. Therefore, all things being considered, the conclusion that RX J0059.2−7138 contains a highly luminous, extreme ultrasoft X-ray spectral component is nearly inescapable. The blackbody radii corresponding to the L_{BB} values quoted in Table 1 are $6^{+19}_{-4} \times 10^9$ cm. Finally, I note that the power-law index is slightly steeper than expected based on extrapolating the spectral shape derived from 2–10 keV band observations of other X-ray pulsars.

A spectrum of the pulsed emission was made from phase bins 3–7 (see Fig. 1) using phase bins 1–2 and 8–10 for background. A single absorbed power law was an excellent fit to these data, $\chi^2 = 25.35$ for 24 degrees of freedom (confidence level for rejection being merely 61%). Both the line-of-sight column density, $N_{\rm H} = 0.6^{+1.9}_{-0.4} \times 10^{21}$ cm^{-2}, and the power-law index, $\alpha_P = 1.0^{+1.0}_{-0.7}$, were consistent with the values from the phase-averaged spectrum. The lack of an EUS spectral component to the pulsed emission is consistent with the lack of observed modulation in the lowest PSPC band and supports the conclusion that the EUS component is nearly unpulsed.

The nearest known X-ray source to the position of RX J0059.2−7138 is the EUS source 1E0056.8−7154 discovered by the *Einstein Observatory* (Seward & Mitchell 1981; Bruhweiler et al. 1987; Wang & Wu 1992). This source was detected in both the *ROSAT* all sky survey (Kahabka & Pietsch 1993) and in PSPC pointed observations (Pietsch & Kahabka 1993). I, too, clearly detect it about 4′ northwest of the new transient at a counting rate of 0.372 ± 0.011 s^{-1}. Its usefulness to the current analysis rests mainly on the independent check it provides for the procedure used to determine the position of RX J0059.2−7138. The position of 1E0056.8−7154 derived from the PSPC data, after correcting for the three effects listed above, is within 5″ of the HRI position. This agreement verifies the procedure used to determine accurate positions of off-axis sources in this PSPC field and establishes the level of positional accuracy obtained.

This source is indeed soft: there are almost no photons detected above an energy of 0.5 keV. A fit of a blackbody spectrum to the PSPC data yields a temperature of $kT_{BB} = 24$ eV and column density of 4.4×10^{20} atoms cm^{-2} for a source at a distance of 57.5 kpc emitting at the Eddington luminosity ($\sim 10^{38}$ ergs s^{-1}) for a 1.4 $M_\odot$ object. Comparison to the *Einstein* IPC and HRI data from 1979 and 1980 indicates possible long-term variability at the level of 20%–40%. These characteristics are very similar to those from other EUS sources in the LMC (Greiner et al. 1991).

3. DISCUSSION

Most known X-ray pulsars in binaries occur in high-mass systems, *i.e.*, where the companion is an O or B star. These systems also show transient X-ray outbursts and flaring behavior on timescales of minutes. Since RX J0059.2−7138 displays all these properties, I tentatively identify it as a high-mass X-ray binary and perhaps even a Be/X-ray binary. This would suggest that the optical counterpart is indeed the 14.1 mag HST guide star mentioned above. The brightness of this star is similar to that of other optically identified high-mass X-ray binaries in the Magellanic Clouds and would indicate a spectral type around B0 (for luminosity classes III–V). Narrow-band optical images of this part of the SMC from an observing session at the CTIO Schmidt telescope on 1993 December 11 indicate the presence of Hα emission from the star at a level of about 15 Å equivalent width (R. C. Smith, 1994 private communication). Additional optical follow-up observations of the proposed counterpart, which should be able to confirm the identification, are underway.

The new SMC transient shares some characteristics of its X-ray emission with the well-studied Galactic low-mass X-ray binary, Her X-1. Like RX J0059.2−7138, Her X-1 is a short period (1.24 s) X-ray pulsar. Perhaps one of the most interesting and relevant features of the X-ray emission of Her X-1 is the highly luminous EUS spectral component ($kT_{BB} \sim 100$ eV) which it shows during high state (Shulman et al. 1975; Catura & Acton 1975). This intense soft X-ray emission has been attributed to reprocessing of the hard X-ray emission from the neutron star surface by either (1) an opaque partial shell of gas near the Alvén radius (Basko & Sunyaev 1976; McCray & Lamb 1976) or (2) the inner edge of an accretion disk (McCray et al. 1982). The latter scenario was motivated by detailed measurements of the pulse profile of Her X-1, which indicated strong modulation (~50%–100%) in the soft X-ray pulse waveform, shifted in phase relative to the hard X-rays.

Strong modulation is clearly not observed in the soft X-ray flux of RX J0059.2−7138, and in this respect then, it is more similar to the several "pure" EUS sources seen in the Magellanic Clouds, such as CAL 83, CAL 87, RX J0527.8−6954, and the EUS source 1E0056.8−7154 mentioned above. One of the models which may explain the soft X-ray emission from these sources is similar to the opaque partial shell model for Her X-1 mentioned above, in that it entails reprocessing of harder X-rays from the central accreting source. In this case, a compact object is shrouded by massive accretion, and the soft X-ray emission arises from the Compton scattering of harder X-rays from near the surface of the accreting object by a surrounding cocoon of ionized matter (Ross 1979). Furthermore, as shown by Kylafis & Xilouris (1993), models of this type for the EUS sources can be made consistent with unified models for low-mass X-ray binaries. For RX J0059.2−7138, any possible surrounding opaque shell surely must be partial, since I see the harder pulsed X-ray emission, which shows no evidence for intrinsic absorption, from near the neutron star's surface. Indeed, the challenge to understanding the X-ray emission from RX J0059.2−7138 in the context of this model rests on finding a geometry for the partial shell which would provide both the broad pulse seen in the hard X-rays but which would also produce little or no modulation in the EUS X-ray flux.

It is clear that the competing theory for the EUS sources in which the soft X-ray emission arises from steady thermonuclear burning of hydrogen on the surface of a white dwarf accreting from a main-sequence companion (van den Heuvel et al. 1992) cannot be an explanation for the soft emission from either Her X-1 or RX J0059.2−7138. One of the motivations for this attractive model arose from the concern that accreting neutron stars or black holes would be unable to reprocess the hard radiation from the central star into the soft X-ray band. The discovery of an EUS X-ray spectral component in an accretion powered neutron star system, as presented here, indicates that such reprocessing is not only possible but evidently occurs in nature. It remains to be seen whether or not this discovery weakens support for the accreting white dwarf model as a description of the pure EUS sources.

ACKNOWLEDGEMENTS

I thank Paul Callanan, Josh Grindlay, Jeff McClintock, Saul Rappaport, and Pat Slane for helpful discussions. This research was partially supported by NASA under the *ROSAT* Guest Observer Program.

REFERENCES

Balucinska-Church, M., & McCammon, D. 1992, ApJ, 400, 699

Basko, M. M., & Sunyaev, R. A. 1976, MNRAS, 175, 395

Bruhweiler, F. C., Klinglesmith, D. A., Gull, T. R., & Sofia, S. 1987, ApJ, 317, 152

Catura, R. C., & Acton, L. W. 1975, ApJ, 202, L5

Clark, G., Doxey, R., Li, F., Jernigan, J. G., & van Paradijs, J. 1978, ApJ, 221, L37

Cowley, A. P., Schmidtke, P. C., Hutchings, J. B., Crampton, D., & McGrath, T. K. 1993, ApJ, 418, L63

Fabian, A. C., Guilbert, P. W., & Callanan, P. J. 1987, MNRAS, 225, 29p

Greiner, J., Hasinger, G., & Kahabka, P. 1991, A&A, 246, L17

Hindman, J. V. 1967, Australian J. Phys., 20, 147

Hodge, P. W., & Wright, F. W. 1977, The Small Magellanic Cloud (University of Washington Press)

Jones, L. R., Pye, J. P., McHardy, I. M., & Fairall, A. P. 1985, Spa. Sci. Rev., 40, 693

Kahabka, P., & Pietsch, W. 1993, in New Aspects of Magellanic Cloud Research, eds. B. Baschek, G. Klare, & J. Lequeux (Berlin: Springer-Verlag), 71

Kylafis, N. D., & Xilouris, E. M. 1993, A&A, 278, L43

Long, K. S., Helfand, D. J., & Grabelsky, D. A. 1981, ApJ, 248, 925

McCray, R. A., & Lamb, F. K. 1976, ApJ, 204, L115

McCray, R. A., Shull, J. M., Boynton, P. E., Deeter, J. E., Holt, S. S., & White, N. E. 1982, ApJ, 262, 301

Morrison, R., & McCammon, D. 1983, ApJ, 270, 119

Orio, M., & Ögelman, H. 1993, A&A, 273, L56

Pietsch, W., & Kahabka, P. 1993, in New Aspects of Magellanic Cloud Research, eds. B. Baschek, G. Klare, & J. Lequeux (Berlin: Springer-Verlag), 59

Raymond J. C.,& Smith, B. W. 1977, ApJS, 35, 419

Ross, R. R. 1979, ApJ, 233, 334

Russell, S. C., & Dopita, M. A. 1992, ApJ, 384, 808

Schaeidt, S., Hasinger, G., & Trümper, J. 1993, A&A, 270, L9

Seward, F. D., & Mitchell, M. 1981, ApJ, 243, 736

Shulman, S., Friedman, H., Fritz, G., Henry, R. C., & Yentis, D. J. 1975, ApJ, 199, L101

Trümper, J., et al. 1991, Nature, 349, 579

van den Bergh, S. 1989, A&A Rev, 1, 111

van den Heuvel, E. P. J., Bhattacharya, D., Nomoto, K., & Rappaport, S. A. 1992, A&A, 262, 97

Wang, Q., Hamilton, T., Helfand, D. J., & Wu, X. 1991, ApJ, 374, 475

Wang, Q., & Wu, X. 1992, ApJS, 78, 391

White, N. E., Nagase, F., & Parmar, A. N. 1994, in X-ray Binaries, eds. W. H. G. Lewin, J. van Paradijs, & E. P. J. van den Heuvel (Cambridge: Cambridge University Press), in press

TABLE 1
Two-Component Spectral Model Fits to
Pulse-Phase–Averaged PSPC Spectrum

Parameters	Best-Fit values [a]
$N_{\rm H}$ (atoms cm^{-2})	$(8.8^{+2.7}_{-2.1}) \times 10^{20}$
$F_{1\,\rm keV}$ [b] (photons s^{-1} cm^{-2} keV^{-1})	$(3.89^{+0.34}_{-0.26}) \times 10^{-2}$
α_P	$2.44^{+0.19}_{-0.16}$
L_{BB} [c] (ergs s^{-1})	$(6.7^{+43.1}_{-5.4}) \times 10^{38}$
kT_{BB} (eV)	$35.6^{+8.5}_{-7.2}$
χ^2 (d.o.f.)	22.68 (22)

[a] Statistical errors at 90% confidence.
[b] Flux density of power-law model at 1 keV.
[c] Bolometric luminosity of blackbody assuming a distance of 57.5 kpc.

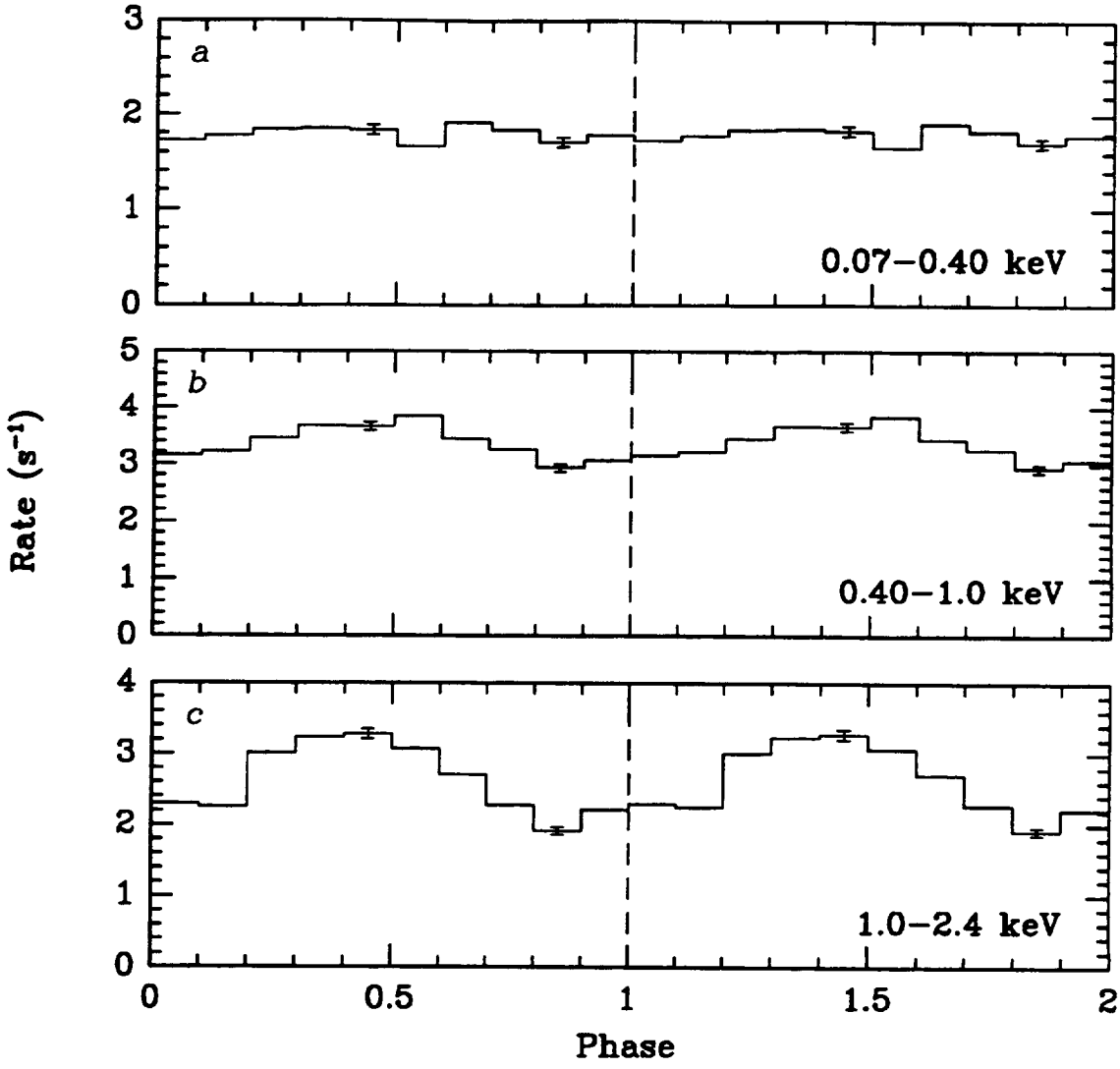

FIG. 1.–The pulse profile of RX J0059.2−7138 folded modulo the pulse period (2.7632 s) for three different energy ranges: 0.07–0.40 keV (*a*), 0.40–1.0 keV (*b*), and 1.0–2.4 keV (*c*). In each panel two complete cycles are shown. The data have been background subtracted and exposure corrected.

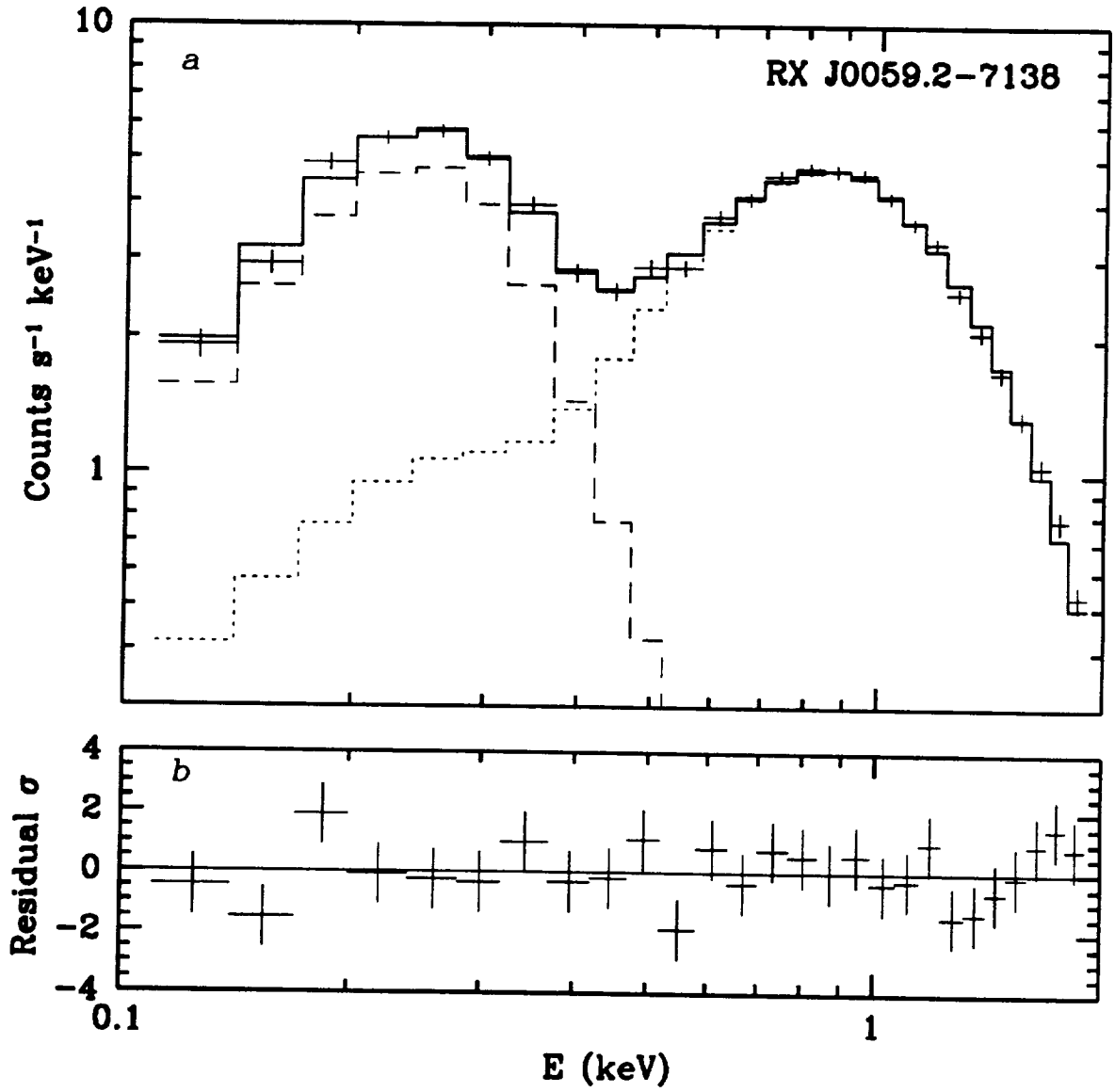

FIG. 2.—(*a*) The pulse-phase–averaged PSPC spectrum of RX J0059.2−7138 with the best-fit two component model. The individual spectral components are shown as the dashed (blackbody) and dotted (power-law) histograms. (*b*) The difference between the observed data and the best-fit model expressed in terms of the statistical error in each energy channel.

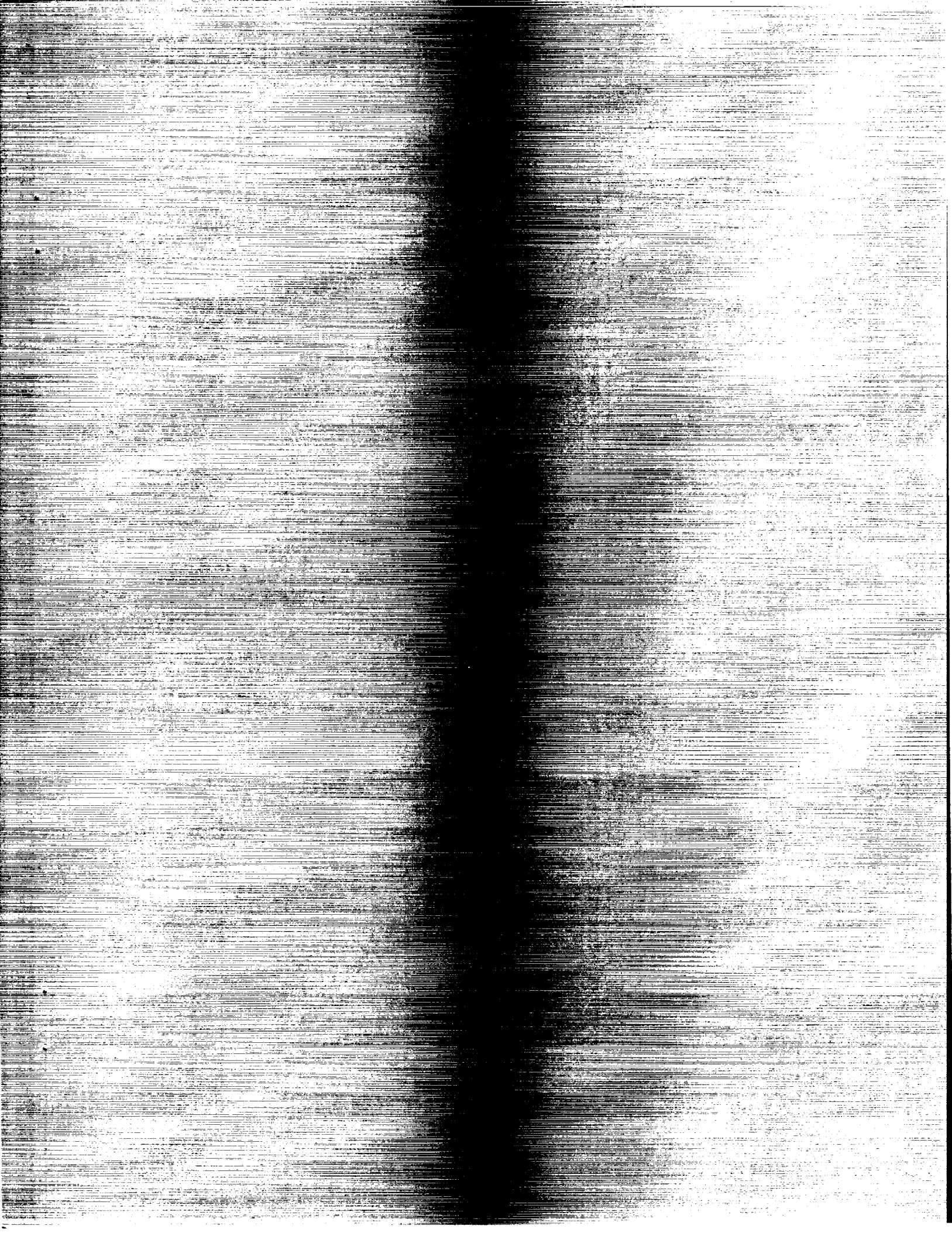

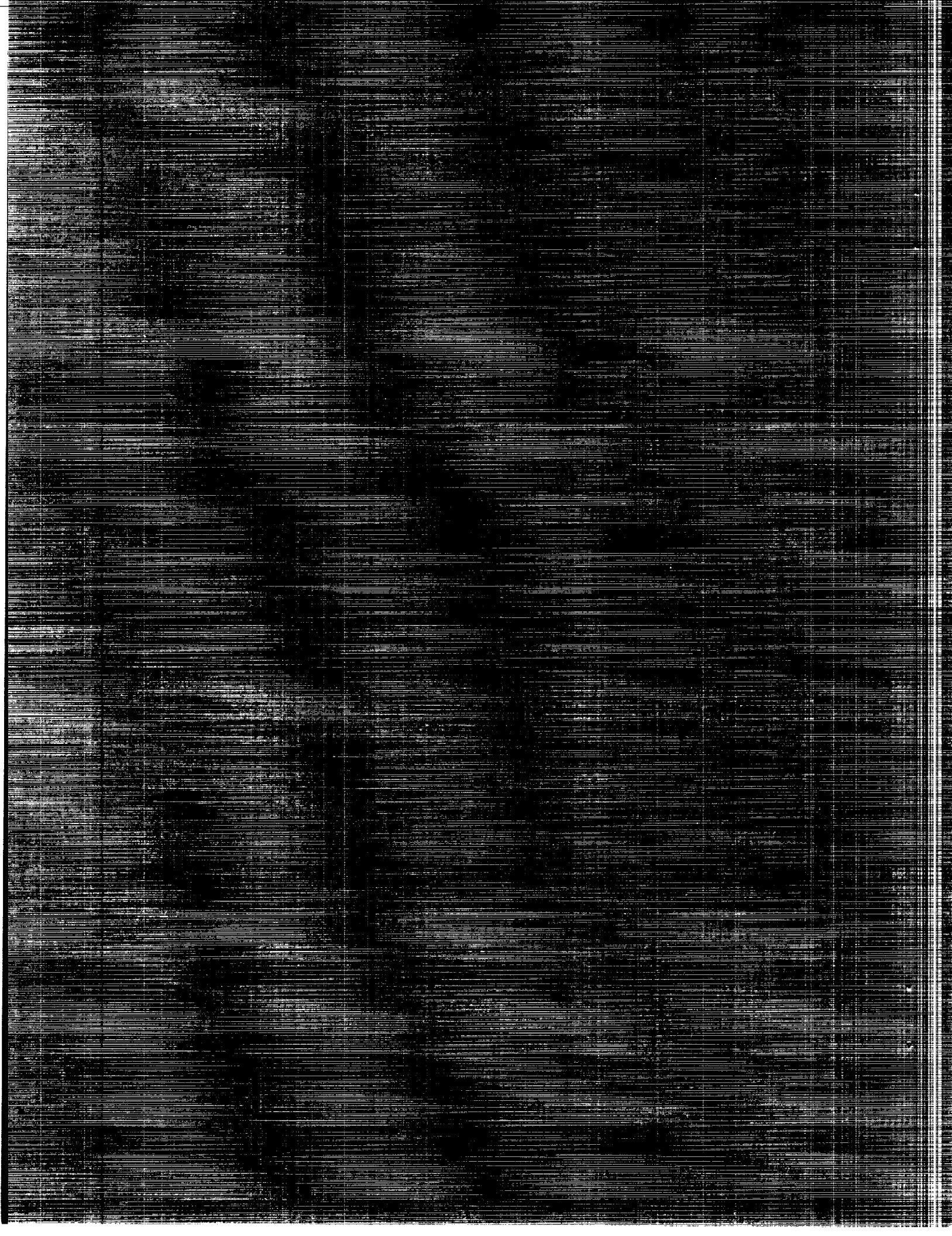

74.11

HEAO-1 A2 Maps of the Hard X-ray Sky

K.Jahoda, J.S.Allen, L.A.Whitlock (NASA/GSFC)

We present maps of the hard X-ray (2-20 keV) sky in four overlapping energy bands. The data are from the HEAO-1 A2 all sky scanning experiment. Though these data were collected in 1977-79, this survey remains unequalled by any other existing or approved mission. We discuss public access to these data (through the GSFC High Energy Astrophysics Science and Archival Research Center) and issues related to use of these data including exposure, statistical and systematic uncertainties, point source response function, and energy response.

74.12

***ASCA* Observations of the Cool Cluster A262**

R.E. White III (Univ. of Alabama), C.S.R. Day (NASA/GSFC/USRA)

ASCA spectral analysis of the cool galaxy cluster A262 will be presented. Constraints on the abundances of individual elements will be discussed in the context of discriminating between various galactic metal ejection mechanisms.

74.13

A New X-Ray–Discovered Cluster of Galaxies Associated with CL0016+16

J.P. Hughes, M. Birkinshaw, J.P. Huchra (SAO)

We have discovered a new cluster of galaxies, RX J0018.3+1618, in a deep ROSAT PSPC pointing of the distant cluster CL0016+16. The X-ray flux of the new cluster is 8×10^{-14} ergs s^{-1} cm^{-2} in the 0.2–2 keV band, which is about 10% of the X-ray flux of CL0016+16. We carried out optical spectroscopy at the Multiple Mirror Telescope and measured the redshifts of 10 galaxies in the direction of RX J0018.3+1618. Eight galaxies lie at a redshift of $\sim$0.55. The difference in mean radial velocity between the new cluster (z=0.5498) and CL0016+16 (z=0.5455) is comparable to the internal velocity dispersions of the clusters. The angular separation between them is 10′ corresponding to a linear distance of 4.4 Mpc for a Hubble constant of 50 km s^{-1} Mpc^{-1} and $q_0=0.5$. We investigate the likelihood that these clusters are bound and speculate on the implications of this discovery for models of large scale structure.

74.14

Cluster X-Ray Substructure and Radio Galaxy Correlations

M.J. Ledlow and J.O. Burns (New Mexico State University)

Current wisdom suggests that X-ray substructure in the intracluster medium (ICM) is fairly common in galaxy clusters. This substructure takes the form of elongations, isophotal twisting, asymmetries, and subclumping. Substructure is also frequently present in kinematical analysis of the galaxy velocity and spatial distributions. These features include bimodality, kurtosis or skewness, and non-Gaussian velocity distributions. Consistent with the observations, Hydro/N-Body simulations suggest that cluster-subcluster mergers may be the culprit to explain these features in the ICM gas distribution, and would indicate that many clusters, even at the present epoch, are still undergoing significant dynamical evolution.

From a sample of X-ray images from the Einstein satellite and, more recently, the ROSAT mission, Burns *et al.* (1994) found a significant correlation between the positions of radio galaxies and subclumps within the cluster-scale X-ray emission. Burns *et al.* have suggested that radio galaxies reside in the residue of cluster/sub-cluster merging sites, and may therefore act as pointers to clusters with ongoing and intersting dynamical activity. We are following up these ideas with a detailed substructure analysis, and a comparison to a sample of clusters without radio galaxies.

In order to determine the signficance of substructure, we have reanalyzed the X-ray images using a Bootstrap-Resampling Monte-Carlo technique. In this method, asymmetries, elongations, and other forms of substructure are evaluated using a moment-analysis similar to Möhr *et al.* (1994), with the advantage that we need not assume apriori any specific substructure-free model for the source (i.e. a Beta-model). The significance of individual features is determined solely from a comparison to statistical fluctuations (including noise) of the actual data. Using this technique, we place limits on the fraction of clusters with significant substructure and test the radio galaxy/substructure correlations from our radio-loud and quiet samples.

74.15

X-ray Cluster Evolution and Projection Effects in a CHDM Universe

C. Loken, A. Klypin, J. Burns (NMSU), G. Bryan, M. Norman (U. Illinois, NCSA)

We have generated surface-brightness projections of large-scale structure simulations (at different epochs) in the *Einstein* and ROSAT bandpasses in order to calculate the probabilities of misidentifying filaments and projected groups as rich clusters. Cluster masses are tracked as a function of time in order to estimate cluster merger and mass accretion rates. We also show how cluster profiles vary with time and fit King models to the cold, hot and baryonic components in order to estimate core radii and slopes. The particular simulations used for this analysis self-consistently evolve both baryons (gas) and dark matter in a CHDM universe. The X-ray properties of the resulting clusters have already been shown to agree well with observational results (Bryan et. al 1994).

74.16

ROSAT Observations of Clusters in Bimodal Systems

M.J. Henriksen (University of Alabama)

We present results from an analysis of bimodal clusters observed with the ROSAT PSPC. The isothermal temperatures are poorly constrained but are roughly, 2 - 4 keV, consistent with that expected from the luminosity-temperature relationship for rich clusters extrapolated to the bimodal cluster luminosities. These are the first temperatures measured for subclusters in bimodal systems. The isothermal masses, $\simeq 4\times10^{14} M_{\odot}$, are much smaller than those derived from rich evolved clusters and are roughly equal in a pair. Comparison to simulations of cluster formation indicates that they are the final stage before a rich cluster is formed by merger. Preliminiary analysis shows that the cooling times appear to be long compared to the age of the clusters, implying that the subclusters do not have cooling flows. The gas density profile is used together with the temperature profile to make the first measurements of the gas baryon fraction for this class of objects. We find that the average gas baryon fraction has a lower limit of $\simeq$25%, consistent with that found for rich clusters of galaxies.

74.17

Diffuse X-ray Emission in Groups of Galaxies

J. S. Mulchaey (OCIW), D. S. Davis (U. of Alabama), R. F. Mushotzky (NASA/GSFC), D. Burstein (Arizona State University)

Diffuse x-ray emission has now been discovered in over a dozen poor groups of galaxies with the ROSAT PSPC. The temperature of the x-ray emitting gas is $\sim$ 1 keV, with low metal abundances implied in some cases. These properties are similar to those found in the NGC 2300 group. Under the assumption that the gas is in hydrostatic equilibrium, the x-ray observations can be used to estimate the total masses of these systems. We provide a summary of the x-ray and optical properties of x-ray detected groups and compare them to clusters of galaxies.

H rd- sonian
Ce for rophysics

(Rece)

A NE ISC USTER OF GALAXIES
OOL 0016+16

J s, Mar and John P. Huchra
Smithso Astrophysics

Astro (Letters)

HARVARD COLLEG RY ITHSONIAN ASTROPHYSICAL OBSERVATORY
treet, C achusetts 02138

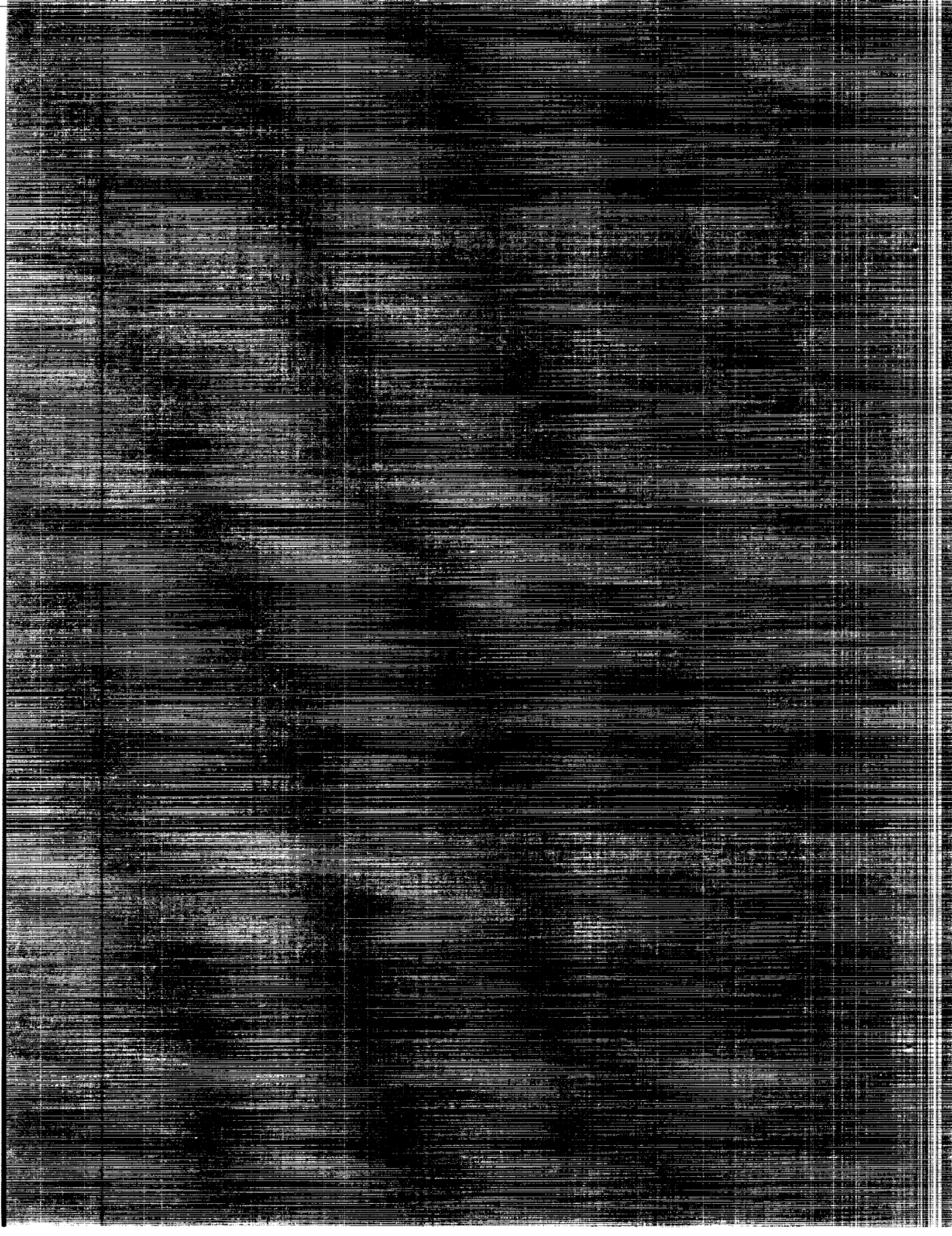

Center for Astrophysics
Preprint Series No. 4116

A New X-ray–Discovered Cluster of Galaxies Associated with CL 0016+16[1]

John P. Hughes,[2] Mark Birkinshaw,[3] and John P. Huchra
Harvard-Smithsonian Center for Astrophysics
60 Garden Street, Cambridge, MA 02138

To appear in *The Astrophysical Journal Letters*
August 1, 1995

Received: 17 April 1995
Accepted: 24 May 1995

Subject headings: cosmology: observations – galaxies: clusters: individual (CL 0016+16, RX J0018.3+1618) – large-scale structure of universe

---

[1] Optical observations reported here were obtained at the Multiple Mirror Telescope, a joint facility of the Smithsonian Institution and the University of Arizona.

[2] E-mail: jph@cfa.harvard.edu

[3] Also Department of Physics, University of Bristol, Bristol, BS8 1TL, UK

ABSTRACT

We have discovered a new cluster of galaxies, RX J0018.3+1618, in a deep ROSAT PSPC pointing toward the distant cluster CL 0016+16. The mean radial velocities of the new cluster (z=0.5506) and CL 0016+16 (z=0.5455) differ by 1000 ± 390 km s^{-1}, which is comparable to their internal velocity dispersions. The angular separation of the clusters, 9.5′, corresponds to a projected linear distance of 4.2 Mpc. RX J0018.3+1618 has an X-ray luminosity in the 0.2–2 keV band of 1.3×10^{44} ergs s^{-1}, which is about 10% of the luminosity of CL 0016+16. From the redshifts of seven galaxies in the new cluster, we derive a radial velocity dispersion of 540^{+260}_{-120} km s^{-1}, which establishes RX J0018.3+1618 as one of the most distant known poor clusters. Simple energetic arguments suggest that the two clusters constitute a bound system. This discovery adds considerable weight to the suggestion made by Koo in 1981 that CL 0016+16 is part of a massive large-scale structure at $z \sim 0.55$.

1. INTRODUCTION

Redshift surveys covering large areas of the sky (*e.g.*, Kirshner *et al.* 1981; de Lapparent, Geller, & Huchra 1986) have revealed a wealth of detail about the nearby, $z < 0.1$, Universe. The picture that emerges has galaxies arrayed in clusters and superclusters on shell-like structures surrounding large voids (Rood 1988). The scales of the observed structures are comparable to the depths of the surveys: for example, the 'Great Wall' (Geller & Huchra 1989) is estimated to be 170×60 Mpc in size (adopting $H_0 = 50$ km s^{-1} Mpc^{-1}, $q_0 = 0.5$ as throughout the present Letter). Considerably less is known about the structure of the Universe at $z > 0.2$, although deep pencil-beam surveys (*e.g.*, Broadhurst *et al.* 1990) have revealed indications of (possibly periodic) large scale structures in the redshift distribution of galaxies up to $z \sim 0.5$.

Koo (1981, 1986) used multicolor data to estimate the redshifts of galaxies in distant large scale structures. Of particular relevance to our work here is his suggestion, based on study of Selected Area 68, that the rich, distant cluster of galaxies CL 0016+16 may be a member of a supercluster at redshift 0.54. In addition to finding CL 0016+16 itself (Koo 1981), Koo found that the distribution of over 300 galaxies, with red colors that correspond to redshift range 0.4–0.6, are more clustered than a control sample of galaxies with random colors. Three of the red galaxies have spectroscopic redshifts of 0.535, 0.540, and 0.540 (Koo 1985), similar to the systemic redshift of CL 0016+16 ($z = 0.5455$, Dressler & Gunn 1992).

We observed CL 0016+16 with the ROSAT Position Sensitive Proportional Counter (PSPC), as part of a project to characterize the density and temperature structure of clusters with well-measured Sunyaev-Zel'dovich decrements (Hughes & Birkinshaw 1995). During the analysis of these data we found a second cluster in the field. The present Letter presents our analysis of the X-ray data for this object, describes the optical work that confirmed its reality, and explores the possibility that the new cluster is bound to CL 0016+16 and may be part of a larger structure.

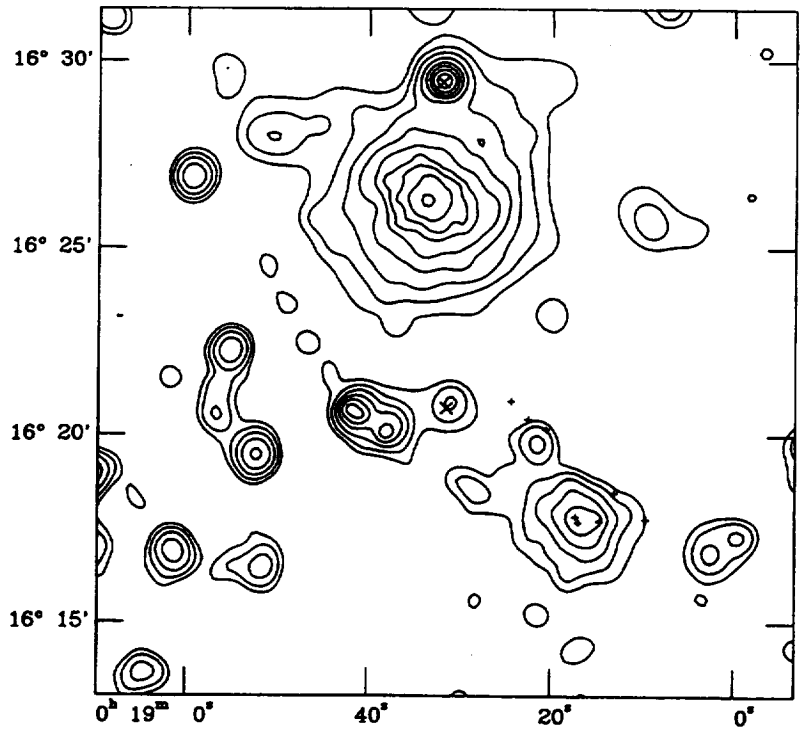

FIG. 1.—A portion of the 0.4-2.4 keV ROSAT PSPC X-ray image containing CL 0016+16 (centered at $00^h18^m33.2^s$, 16°26′18″) and RX J0018.3+1618 (centered at $00^h18^m16.8^s$, 16°17′45″). Coordinates are in epoch J2000. The data have been background subtracted, exposure corrected, and adaptively smoothed. Contour levels start at 1.8×10^{-4} counts s^{-1} arcmin^{-2} (~30% of the average background level) and increase by multiplicative factors of 1.937. The crosses mark the optical (or radio) positions of two (out of five) candidate counterparts to the X-ray sources used for boresight correction. The plus signs indicate the positions of the eight galaxies for which we have measured redshifts of $z \sim 0.5$.

2. OBSERVATIONS

2.1. X-Ray

Our data came from a 43,157 s PSPC observation carried out during 1992 July. Figure 1 shows a central portion of the field after background subtraction and exposure correction. The data were smoothed with an intensity-dependent smoothing kernel, a Gaussian with standard deviation increasing from 7.5″ to 1′ as the brightness decreases from the brightest to the dimmest regions on the image. This preserves structure on all relevant scales in CL 0016+16. A boresight correction was applied to the data, which was based on a comparison of the known positions of five sources (three *HST* guide stars, one radio source, and one active galactic nucleus) with the positions of their apparent X-ray associations. The ~8″ correction has an uncertainty of <3″ in each coordinate.

Many unresolved serendipitous sources appear in the ROSAT field, but one object, 9.5′ southwest of CL 0016+16, appears extended. Indeed, a fit of a point source, employing the appropriate off-axis radially averaged point-spread function (Hasinger *et al.* 1994), is unacceptable (reduced $\chi^2_\nu = 4.7$ for $\nu = 22$ degrees of freedom). An acceptable fit

($\chi^2_\nu = 1.1$ for $\nu = 20$) is obtained using an intrinsic surface brightness profile of the form $\Sigma = \Sigma_0[1+(\theta/\theta_C)^2]^{-3\beta+0.5}$, the so-called isothermal-β model for galaxy clusters (Cavaliere & Fusco-Femiano 1976). The best-fit values, $\beta = 0.72^{+0.20}_{-0.11}$, $\theta_C = 0.44^{+0.22}_{-0.14}$ arcmin, and $\Sigma_0 = (9.6^{+3.5}_{-2.4}) \times 10^{-3}$ counts s^{-1} arcmin^{-2}, are consistent with those expected from a distant cluster of galaxies. The (boresight-corrected) center of the isothermal-β model (from maximum likelihood fits to the image) is $00^h18^m16.8^s$, 16°17′45″ (J2000) with an uncertainty of less than 4″ in each coordinate. We detect roughly 320 photons from the candidate cluster within a radius of 3′. Spectral analysis shows that the X-ray data are consistent with the Galactic column 4.1×10^{20} atoms cm^{-2} and a temperature $\gtrsim$1.5 keV (observed frame). The X-ray flux in the 0.2–2.0 keV band is 8.3×10^{-14} ergs s^{-1} cm^{-2}.

2.2. Optical Imaging

We observed the candidate cluster with the 1.2-m telescope at the Whipple Observatory on 1993 October 23 under photometric conditions. The focal plane detector (a Ford 2048 × 2048 CCD) was binned to produce an effective pixel scale of 0.65″. Two 900 s exposures in R were taken. Using standard IRAF tasks, we bias-subtracted the data, eliminated cosmic rays and bad pixels, and flat-fielded with a twilight sky exposure. The residual spatial structure in the background on our source exposures was removed by subtracting a two-dimensional low-order polynomial surface. The image was registered to the celestial sphere to a positional uncertainty of $\lesssim$1″ using the positions of five *HST* guide stars. The plate scale was accurately determined using a short (20 s) exposure of M67, which also served to provide photometric standards (Schild 1983).

Figure 2 (Plate L00) shows a portion of the R-band image. Numerous faint galaxies are associated with the diffuse X-ray emission, with a dominant bright galaxy (labeled 1) within 12″ of the center of the X-ray emission. These optical data strongly support the identification of the extended X-ray source as a cluster of galaxies.

A moment analysis (determining centroid, FWHM, and ellipticity) was performed on about 100 objects (selected by eye) to identify candidates for follow-up optical spectroscopy. Due to the limited seeing (about 2″), the relatively large size of the image pixels and the faintness of the objects, we did not use the derived shape parameters in choosing candidates. Rather, we restricted ourselves to objects within 2 mag of the central bright galaxy ($19.5 < m_R < 21.5$). We were further restricted in our choice of spectroscopic targets by constraints associated with the aperture plate layouts. In Figure 2 we indicate by numerical label the eight galaxies for which follow-up spectroscopy indicates redshifts of ∼0.5. The positions of these galaxies are also marked on the X-ray map (Fig. 1). Other objects for which optical spectra were obtained are indicated by alphabetic labels. Tables 1 and 2 provide the positions and R-band magnitudes (from a fixed 6″ diameter aperture)

TABLE 1
RX J0018.3+1618 SPECTROSCOPIC RESULTS

	Position (J2000)			
n	R.A.	Decl.	R	z
1	$0^h18^m17.0^s$	16°17′41″	19.5	0.5498 ± 0.0003
2	17.3^s	17′50″	20.4	0.5463 ± 0.0003
3	14.6^s	17′43″	21.5	0.5481 ± 0.0004
4	13.0^s	18′28″	21.5	0.5541 ± 0.0005
5	09.5^s	17′46″	20.9	0.5504 ± 0.0003
6	20.5^s	20′09″	20.7	0.5709 ± 0.0003 [a]
7	22.5^s	20′26″	21.0	0.5529 ± 0.0005
8	24.3^s	20′55″	20.1	0.5529 ± 0.0004

[a] Probable outlier (see text)

TABLE 2
ADDITIONAL SPECTROSCOPIC RESULTS

	Position (J2000)			
n	R.A.	Decl.	R	ID
a	$0^h18^m15.3^s$	16°17′46″	19.8	Galactic star (M0)
b	15.0^s	17′22″	20.0	Galactic star (white dwarf) ?
c	20.0^s	17′56″	21.1	Galactic star (M3)
d	16.9^s	18′33″	21.5	Weak emission line galaxy: $z \sim 0.42$? [a]
e	15.4^s	16′52″	21.1	Galactic star (F subdwarf)
f	20.6^s	17′56″	21.2	Emission line galaxy: $z = 0.1957$ [b]
g	23.2^s	18′08″	21.6	Galactic star (M0)
h	22.1^s	19′09″	20.6	Galactic star (K5)
i	27.4^s	21′12″	20.5	Galactic star (M0)

[a] Tentative redshift from one emission line at 7097 Å
[b] Redshift based on emission lines of Hα, H$\beta$and [O III] $\lambda\lambda$ 4958.9, 5006.9

for the objects indicated in Figure 2 (ordered by increasing angular distance from the central bright galaxy).

2.3. Optical Spectroscopy

We obtained optical spectra of 17 candidate objects at the Multiple Mirror Telescope on 1994 September 7 and 8 using the Red Channel with aperture plates (Fabricant, McClintock, & Bautz 1991). Aperture plates were machined several weeks before the run with slitlets (each 1.5″ × 30″) cut for five objects on each plate, and additional blocked slitlets were used for alignment on bright stars. The detector was a Loral 1200 × 800 CCD binned by 2 on the chip in the spatial (smaller) direction (for a scale of ∼0.6″ pixel^{-1}). We observed using a 270 line mm^{-1} grating blazed at 7300 Å, which provided a spectral resolution of ∼15 Å (FWHM) and a dispersion of 3.6 Å pixel^{-1}. All of the spectra included the wavelength range 5500 – 8500 Å.

We exposed two plates five times for 2700 s each and one plate for three exposures of 2100 s. Air-mass values ranged from 1.0 to 1.8 during the observations. Two 300 s spectra

of two additional objects (labeled a and b) were obtained by blind offset into one of the slitlets during the early part of the second night. He-Ne-Ar lamp exposures were done before and after each exposure and dome flats were done at the beginning or end of the night. The seeing was good ($\sim 1''$) during the run.

Standard IRAF routines were used for the data reduction. Cosmic rays were identified and removed through a comparison of frames. The bias level was subtracted and flat fields were applied. Task APEXTRACT was used to trace and extract the one-dimensional spectra. Wavelength calibration used 20–26 lines from the comparison lamp spectra fit to a cubic spline (rms residuals were ~ 0.5Å). We verified the wavelength of the 6300.2 Å night sky line in our spectra when the data were extracted without sky subtraction. Differences were <1 Å and our derived redshifts were corrected for this shift ($\Delta z \sim 0.0001$). Data from the separate frames were summed after wavelength calibration. The average signal-to-noise ratio in our weakest spectrum was about 15 per spectral resolution element.

Eight spectra clearly showed the H and K lines of Ca II and the 4000 Å continuum break, redshifted to ~ 6200 Å. Accurate radial velocities for these galaxies were determined through cross-correlation techniques over observed wavelength range 5600–7500 Å (task XCSAO) using a spectrum of galaxy NGC 4486B redshifted to $z = 0.55$ as a template. Strong correlations were obtained in all cases, with formal velocity errors 60 – 115 km s^{-1}: the results are given in Table 1. The other nine spectra (Table 2) revealed two emission-line galaxies at redshifts <0.5, five late-type Galactic stars, and a probable F subdwarf. Object b near the cluster core, which was observed only for 600 s, showed a blue, apparently featureless, continuum spectrum and probably corresponds to a white dwarf.

3. DISCUSSION

The mean redshift of the new cluster is 0.5506 ± 0.0012 and the radial component of its velocity dispersion is 540^{+260}_{-120} km s^{-1}, based on seven galaxy redshifts and calculated using the formulae in Danese, De Zotti, & di Tullio (1980). The remaining galaxy (galaxy 6) has a radial velocity more than 7 σ away from the mean; it is likely to be a background galaxy unassociated with RX J0018.3+1618, but possibly related to the larger system. From the correlation between X-ray temperature (kT) and velocity dispersion for nearby clusters (Edge & Stewart 1991b) we estimate $kT \sim 3$ keV for RX J0018.3+1618. This value is consistent with the X-ray spectral fits and with the X-ray luminosity–kT correlation for nearby clusters (Edge & Stewart 1991a). Using this temperature, the imaging results, and the usual assumption of a symmetric, isothermal cluster in hydrostatic equilibrium, we estimate the cluster's mass within a radius of 2 Mpc to be $4.6 \times 10^{14}\ M_\odot$. The ratio of gas mass to total mass within this radius is 13%.

Approximately 9.5′ to the northeast (centered at $00^h18^m33.2^s$, 16°26′18″) lies the rich cluster CL 0016+16. Based on published data (Dressler & Gunn 1992), the redshift of this cluster is 0.5455 ± 0.0016 and its one-dimensional velocity dispersion is 1696^{+291}_{-207} km s^{-1} (these were calculated directly from the individual redshifts given in Table 8 of Dressler & Gunn 1992; due to a numerical error, the velocity dispersions quoted in Table 9 of the same paper are all too low by some 20%–30%, A. Dressler 1995, private communication). The mean temperature of the cluster has been measured by *ASCA* to be $kT = 8.4^{+1.2}_{-0.6}$ keV (Yamashita 1994). The PSPC data for CL 0016+16 can be fitted by an isothermal-β model with $\theta_C \sim 0.70'$ and $\beta \sim 0.74$, although, as Figure 1 clearly shows, the cluster is not axisymmetric and a significantly better fit can be obtained with a model with ellipticity ~0.17. We estimate the mass of CL 0016+16 within 2 Mpc to be $1.3 \times 10^{15}\ M_\odot$, which is ~50% larger than the mass of the Coma Cluster (Hughes 1989). The ratio of gas mass to total mass for CL 0016+16 is 18%.

The redshift of the center-of-mass frame of the two clusters is 0.5468 and the radial velocity difference between them is $v_r = 1000 \pm 390$ km s^{-1}. We study the probability that the clusters are a bound system using a simple energy integral formalism assuming locally flat spacetime and Newtonian gravitation (see Beers, Geller, & Huchra 1982). We represent the relative space velocity between the clusters as $v = v_r / \cos\psi_v$ and the linear distance between them as $d = D_A \theta_p / \sin\psi_d$, expressed in terms of the projection angles (ψ_v, ψ_d) relative to the line of sight, the measured quantities v_r and θ_p (the projected angular separation), and the angular diameter distance D_A. The condition that CL 0016+16 and RX J0018.3+1618 are bound is then $v_r^2 - \frac{2GM}{D_A \theta_p} \sin\psi_d \cos^2\psi_v < 0$. Note that we do not impose the requirement $\psi_v = \psi_d$ that assumes strictly radial motion between the clusters. Figure 3 shows the bound and unbound regions as functions of ψ_d and ψ_v.

The probability that this is a bound system, estimated from the solid angles without regard to other constraints, is 38%. Redshift surveys of clusters of galaxies limit cluster-cluster peculiar velocities to <2000 km s^{-1} (Bahcall, Soneira, & Burgett 1986) and

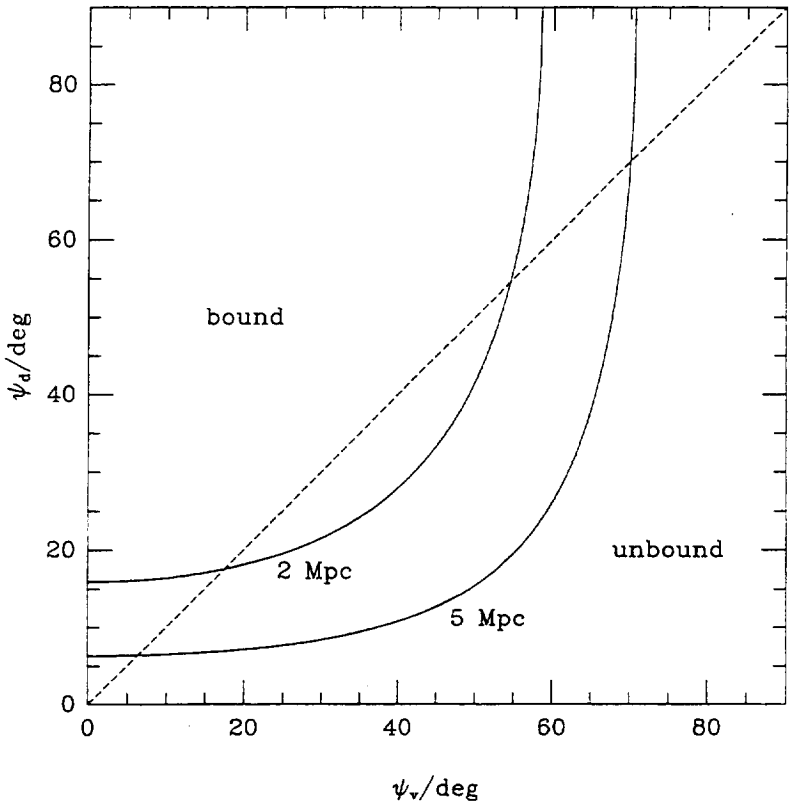

FIG. 3.—Regions of the (ψ_v, ψ_d) plane that correspond to bound and unbound solutions for the derived radial velocity difference v_r = 1000 km s^{-1} and systemic redshift = 0.5468. The two curves correspond to radial limits of 2 and 5 Mpc for the integrated cluster masses, and the dashed diagonal line corresponds to $\psi_d = \psi_v$, the condition of radial motion of RX J0018.3+1618 and CL 0016+16.

probably <1000 km s^{-1} (Huchra *et al.* 1990). Making the conservative assumption that peculiar motions are <3000 km s^{-1}, so that $\psi_v < \cos^{-1}(1/3)$, increases the bound probability to 60%. If we use the cluster masses within 5 Mpc, employing the same technique of mass estimation as above, we obtain the lower curve (marked 5 Mpc) in Figure 3. In this situation the probabilities that the clusters are bound are 58% (all peculiar velocities) and 91% (restricted range of peculiar velocities). From these arguments, we conclude that it is likely (but not necessary) that RX J0018.3+1618 and CL 0016+16 form a bound system.

The complex morphology of CL 0016+16 provides other evidence of dynamical activity. The ellipticities of the isophotes of the X-ray image increase from 0 near the center of CL 0016+16 to a maximum of 0.24 at a radius of 80″ (0.59 Mpc) before decreasing to 0 again at 120″ (0.89 Mpc). Over this radial range the position angle of the major axis is roughly constant at ~50°, but at 120″ it changes abruptly by nearly 90°. From 120″ to 200″ (1.48 Mpc) the ellipticity lies in the range 0.05–0.1. These results bear a striking resemblance to simulations of merging clusters (see Schindler & Müller 1993 in particular). Further support for a recent merger in CL 0016+16 is provided by the distribution of galaxies (Dressler & Gunn 1992), which is consistent with two similar-sized clumps lying 45″ (0.33 Mpc) to either side of the bright central core of the X-ray image. A final indication that CL 0016+16 is not dynamically relaxed comes from a comparison of its velocity

dispersion and gas temperature: the parameter β ($= \mu m_p \sigma^2/kT$) is large ($1.5 \lesssim \beta \lesssim 3.2$) and not $\sim$1 as expected for a relaxed system.

Koo (1981, 1986) has suggested that CL 0016+16 lies in a long, thin filament of galaxies stretching $\sim$25 Mpc to the southwest through Selected Area 68. This is supported by the observed ellipticity of CL 0016+16, which is consistent with a merger of two clusters originally infalling along the axis of the filament, and by the position of RX J0018.3+1618 close to the filament. Furthermore, the discovery of RX J0018.3+1618 highlights the power of deep X-ray images to identify potential wells associated with relatively poor clusters of galaxies at high redshift and thereby to serve as an effective complement to galaxy redshift surveys in mapping large-scale structures.

ACKNOWLEDGMENTS

This research was partially supported by NASA grant NAG5-2156. We thank Dan Fabricant and Doug Mink for helpful discussions.

REFERENCES

Bahcall, N. A., Soneira, R. M., & Burgett, W. S. 1986, ApJ, 311, 15

Beers, T. C., Geller, M. J., & Huchra, J. P. 1982, ApJ, 257, 23

Broadhurst, T. J., Ellis, R. S., Koo, D. C., & Szalay, A. S. 1990, Nature, 311, 726

Cavaliere, A., & Fusco-Femiano, R. 1976, A&A, 49, 137

Danese, L., De Zotti, G., & di Tullio, G. 1980, A&A, 82, 322

de Lapparent, V., Geller, M. J., & Huchra, J. P. 1986, ApJ, 302, L1

Dressler, A., & Gunn, J. E. 1992, ApJS, 78, 1

Edge, A. C., & Stewart, G. C. 1991a, MNRAS, 252, 414

———. 1991b, MNRAS, 252, 428

Fabricant, D. G., McClintock, J. E., & Bautz, M. W. 1991, ApJ, 381, 33

Geller, M. J, & Huchra, J. P. 1989, Science, 246, 897

Hasinger, G., Boese, G., Predehl, P., Turner, T. J., Yusaf, R., George, I. M., & Rohrbach, G. 1994, Legacy, 4, 40

Huchra, J. P., Henry, J. P., Postman, M., & Geller, M. J. 1990, ApJ, 365, 66

Hughes, J. P. 1989, ApJ, 337, 21

Hughes, J. P., & Birkinshaw, M. 1995, in preparation

Kirshner, R. P., Oemler, A., Jr., Schechter, P. L., & Shectman, S. A. 1981, ApJ, 248, L57

Koo, D. C. 1981, ApJ, 251, L75

———. 1985, AJ, 90, 418

———. 1986, ApJ, 311, 651

Rood, H. J. 1988, ARA&A, 26, 245

Schild, R. E. 1983, PASP, 95, 1021

Schindler, S., & Müller, E. 1993, A&A, 272, 137

Yamashita, K. 1994, in New Horizon of X-Ray Astronomy—First Results from *ASCA*, ed. F. Makino & T. Ohashi (Tokyo: Universal Academy), 279

FIG. 2.—R-band image from the Mount Hopkins 1.2 m telescope of a portion of the field containing the new cluster, RX J0018.3+1618. The field of view is approximately 5.5′ square (scale bar is 1′ long) and is centered on position $00^h18^m16.8^s$, 16°19′18″ (J2000); north is up and east is to the left. Contours of constant X-ray surface brightness from Fig. 1 are overlaid. The 8 galaxies for which we measured redshifts of $z \sim 0.5$ (*Table* 1) are numbered. Spectroscopic data were also taken for objects labeled a to i (*Table* 2).

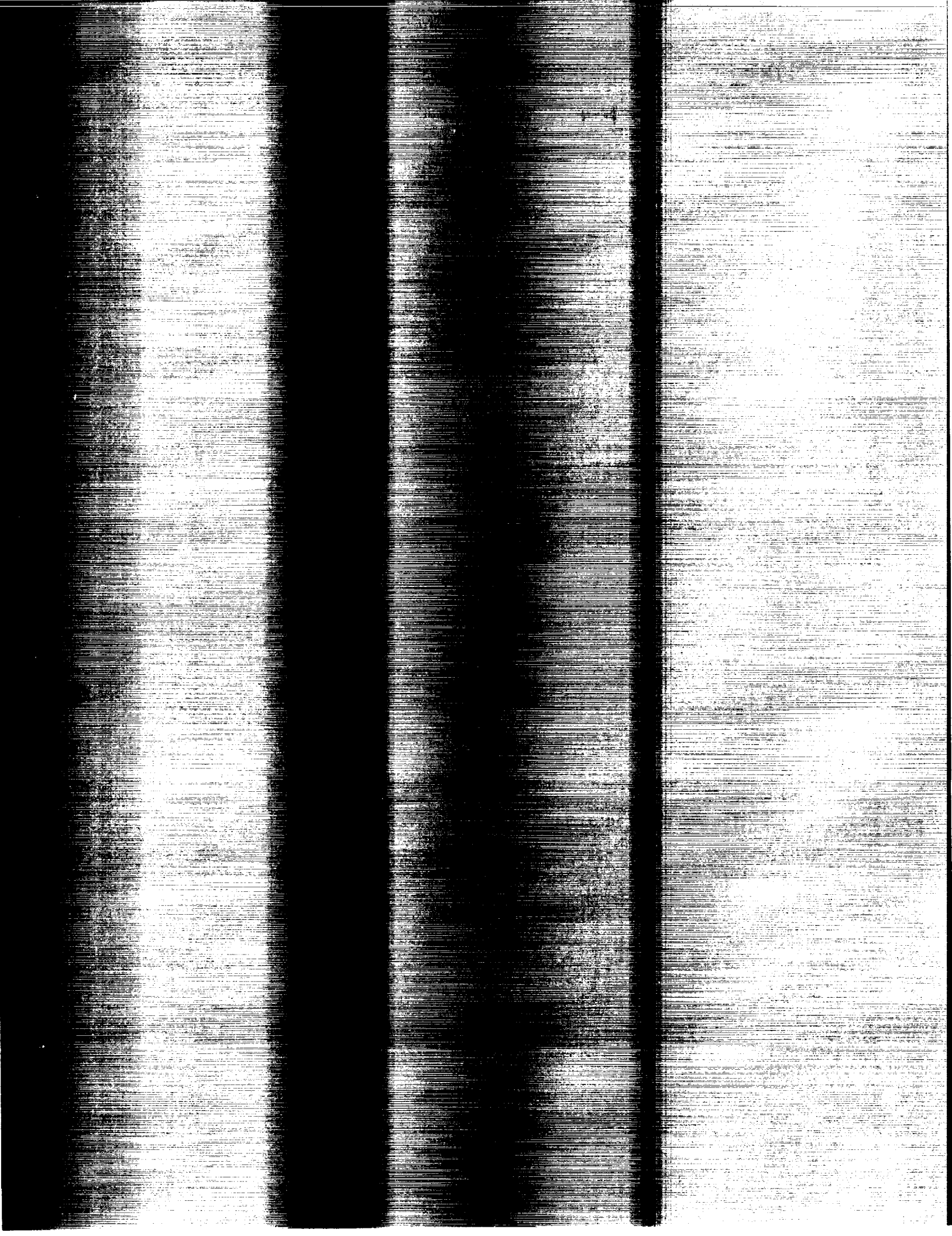

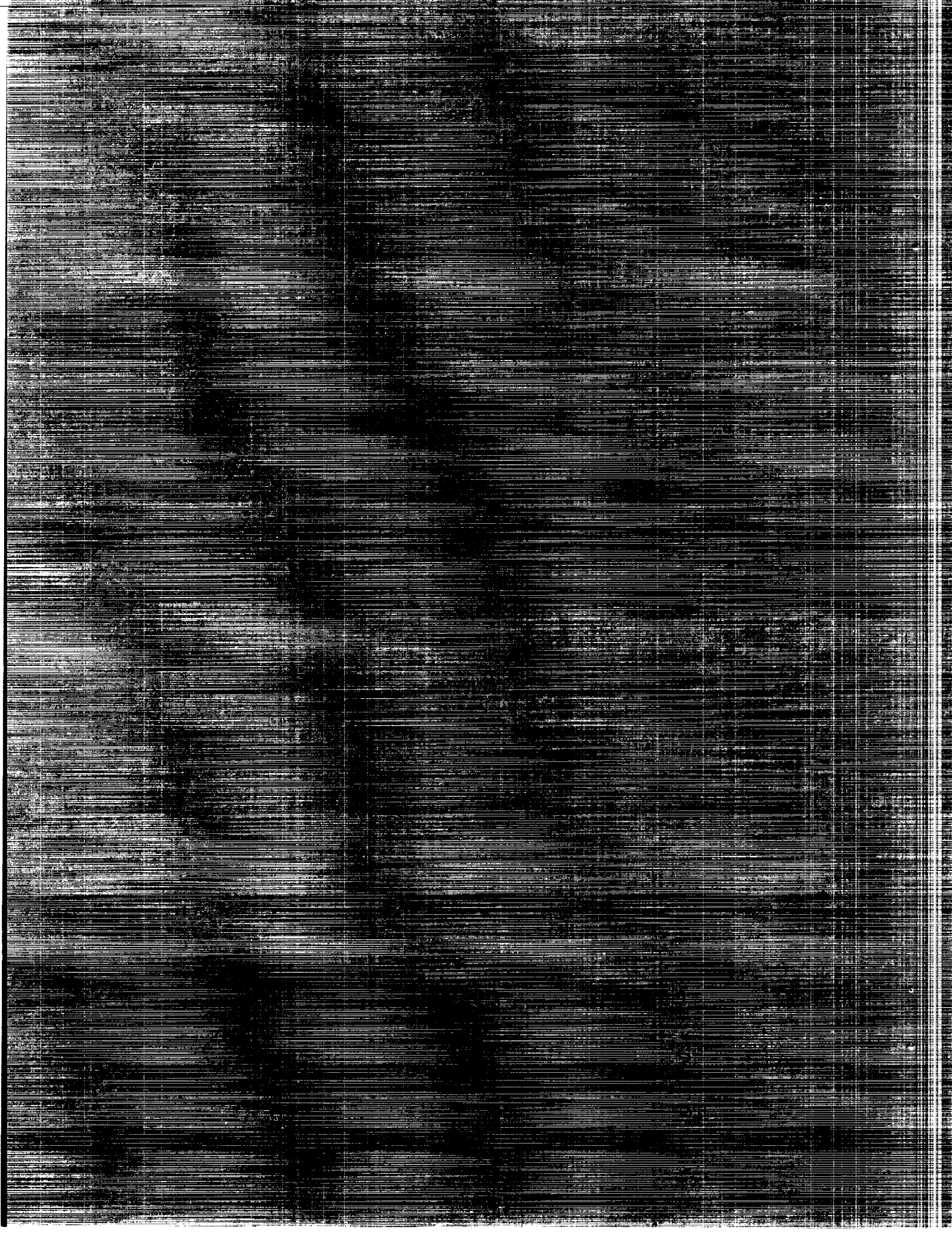

Session 7: Cosmology and Cosmological Parameters
Display Session, 10:00am-6:30pm
Convention Center, North Banquet Hall

7.01

A Measurement of the Angular Power Spectrum of the Anisotropy in the Cosmic Microwave Background

C. B. Netterfield, M. J. Devlin, N. C. Jarosik, L. A. Page (Princeton U.), E. J. Wollack (NRAO)

We report a measurement of the angular power spectrum of the anisotropy in the Cosmic Microwave Background. The anisotropy is measured in 23 different spatial bands (from $\ell_e = 54$ to $\ell_e = 408$) and in 6 frequency bands (from 26 GHz to 46 GHz) over three observing seasons. The frequency spectral index of the fluctuations is consistent with that of the CMB, and inconsistent with either Galactic free-free emission or dust. The measurements are consistent from year to year. Furthermore, the sky coverage of the MSAM experiment (Cheng et al. 1994) was repeated and the results confirmed. The angular power spectrum shows a distinct rise from $ST_l = 49.2^{+7.5}_{-5.0}\mu$K at $\ell = 83$ to $80.4^{+9.5}_{-8.1}\mu$K at $\ell = 234$.

7.02

Uncertainties in the Absolute Age of the Globular Clusters

Brian Chaboyer (CITA), Peter J. Kernan, Lawrence M. Krauss (CWRU), Pierre Demarque (Yale)

As the longstanding discrepancy between the expansion age of the universe and the age of the oldest globular clusters continues, it becomes critically important to provide a realistic estimate of the error associated with the globular cluster age estimates. We report the results of a detailed numerical study designed to answer this question. Utilizing estimates of the uncertainty range (and distribution) in the input parameters of stellar evolution codes we produced 1000 Monte Carlo realizations of stellar isochrones, with which we could determine the ages of the 18 oldest globular clusters using the difference in magnitude between the main-sequence turnoff and the horizontal branch. Incorporating the observational uncertainties in the measured color-magnitude diagrams for these systems and the predicted isochrones, we derived a probability distribution for the mean age of these systems. Our best estimate is 14.6 ± 1.7 Gyr, with the one-sided 95% C.L. lower bound of 12.1 Gyr. The total error budget is dominated by the uncertainty in the absolute magnitude of the horizontal branch. Simply varying this quantity over its full 2σ range, keeping all other parameters fixed, would produce a $\pm 16\%$ change in globular cluster ages estimates. Other significant input parameter uncertainties in this same sense are $[\alpha/\mathrm{Fe}]$ ($\pm 7\%$ effect), mixing length ($\pm 5\%$ effect), and diffusion, ^{14}Np reaction rate, the choice of colour table, and the primordial Helium abundance, each of which would affect age estimates at the $\pm 3\%$ level if allowed to vary over its entire range, keeping all other parameters fixed. Simple formulae are provided which can be used to update our age estimate and its error as improved determinations for the above quantities become available.

7.03

Cosmological Constant and the Graviton Mass

F.C. Michel (Rice Univ., Houston, TX)

The usual choice of sign for the Cosmological Constant (namely, to give repulsion to cancel out the gravitational attraction of the galaxies) seems to correspond to an imaginary mass for the graviton.

7.04

High-Redshift Supernova Searching to Study q_0, Λ, Ω_0, and H_0: First Results from 7 Supernovae at Redshifts $z \sim 0.35$–0.5

A.Kim, S.Deustua, S.Gabi, G.Goldhaber, D.Groom, I.Hook, M.Kim, C.Pennypacker, S.Perlmutter (LBNL/CfPA, Berkeley), A.Goobar (U.Stockholm), R.Pain (IN2P3), R.Ellis, R.McMahon (IoA), B.Boyle, P.Bunclark, D.Carter, M.Irwin (RGO), A.V.Filippenko, T.Matheson (U.C. Berkeley), K.Glazebrook (AAO), M.Dopita, J.Mould (MSSSO, ANU), W.Couch (UNSW), (The Supernova Cosmology Project)

Our search for high-redshift type Ia supernovae has so far discovered seven supernovae. Using a "batch" search strategy, almost all were discovered before maximum light and were observed over the peak of their light curves. The spectra and light curves indicate that almost all were type Ia supernovae at redshifts $z = 0.35 - 0.5$. These high-redshift supernovae can provide a distance indicator and "standard clock" to study the cosmological parameters q_0, Λ, Ω_0, and H_0. This presentation will present observation strategies and rates, analysis and calibration issues, the sources of measurement uncertainty, and some cosmological implications of these first high-redshift supernovae from our ongoing search.

Session 8: Distance Indicators
Display Session, 10:00am-6:30pm
Convention Center, North Banquet Hall

8.01

The Distance to the Cluster of Galaxies Abell 2634

M. Scodeggio, R. Giovanelli, M.P. Haynes (Cornell)

The Tully-Fisher and $D_n - \sigma$ techniques are most commonly used to obtain redshift-independent estimates of galaxy distances. In some cases, however, the two methods yield conflicting results. The most notorious of such cases refers to the cluster of galaxies Abell 2634: while the Tully-Fisher relation applied to a sample of 11 spiral galaxies gave a distance estimate corresponding to essentially zero peculiar velocity, the $D_n - \sigma$ relation applied to a sample of 18 elliptical and lenticular galaxies gave a distance estimate corresponding to a peculiar velocity of -3400 km s^{-1}. This difference has been used as evidence for the possible non-universality of the two relations, which would result in spurious peculiar velocities, and, in turn, in inadequate reconstructions of the local Universe mass density field.

As part of a larger project to compare Tully-Fisher and $D_n - \sigma$ redshift-independent distance estimates for nearby clusters of galaxies, we have obtained I band CCD photometry, and either 21cm line rotational velocities (for spirals) or Mg lines internal velocity dispersions (for E and S0's) for a large sample of galaxies in the region of A2634 (45 spirals and 52 E and S0's). This data-set, combined with a detailed study of cluster membership, is used to obtain an accurate determination of the distance to A2634.

8.02

The Distance to CL0016+16 and the Hubble Constant

J.P. Hughes (SAO), M. Birkinshaw (University of Bristol/SAO)

We use *ROSAT* and *ASCA* X-ray data and Sunyaev-Zel'dovich effect data from the Owens Valley Radio Observatory to estimate the distance to the rich, distant ($z = 0.5455$) cluster of galaxies CL0016+16. We study the sensitivity of the derived value of the Hubble constant to various assumptions about the form of the cluster's three-dimensional density distribution. Specifically we consider (1) spherically symmetric isothermal-β models, (2) purely elliptical isothermal-β models, and (3) a deprojection of elliptical isophotes fitted to the *ROSAT* PSPC data. Results are given for prolate vs. oblate geometries as well as arbitrary line-of-sight inclination angles.

(8)

宇宙圏研究会

平成7年度

X-Ray Imaging and Spectroscopy of Cosmic Hot Plasmas

International Conference on X-Ray Astronomy

—ASCA 3rd Anniversary—

Abstracts

11-14 March, 1996

at Waseda University, Tokyo

宇宙科学研究所

The Expansion of the X-ray Remnant of Tycho's Supernova Remnant (SN1572)

John P. Hughes[1]

[1]Harvard-Smithsonian Center for Astrophysics

The High Resolution Imager (HRI) on *ROSAT* observed Tycho's supernova remnant (SNR) for over 100,000 s in February 1995. This image is about five times deeper than any previous high resolution X-ray image of the SNR and it reveals a number of new spatial features. Most notable is the weak rim of emission seen clearly around the entire remnant, which is believed to be the blast wave propagating through the surrounding circumstellar medium. The brighter regions of the remnant, corresponding to metal-enriched ejecta, are being studied to quantify the amount and size scale of clumping. In this talk, I report on the expansion of the remnant in the X-ray band.

This pointing was the second observation of Tycho's SNR carried out by the *ROSAT* HRI. The first was done in July 1990 for somewhat more than 21,000 s. The time baseline between the two pointings is about 4.5 years, roughly 1% of the age of the SNR, which exploded as a supernova in AD1572. The azimuthally-averaged current expansion rate of Tycho's SNR determined from the two *ROSAT* observations is $0.39''$ yr^{-1}. Dividing the radius of the remnant (roughly $250''$) by the known age (420 yr) gives a mean expansion rate for Tycho of $0.59''$ yr^{-1}. A supernova remnant in the Sedov phase of evolution should show a current expansion rate 0.4 times the time-averaged expansion rate. In the case of Tycho this would suggest a current expansion rate of $0.24''$ yr^{-1}, which is significantly less than what I measure. I conclude that this evidence strongly indicates that Tycho's SNR has not yet entered the Sedov phase of evolution, and that the dynamical evolution is still dominated by the deceleration of reverse-shocked ejecta.

Two small X-ray bright knots in the southeast are particularly interesting, since earlier work (Vancura, Gorenstein, & Hughes 1995) has revealed that these features are almost surely highly enriched knots of SN ejecta with very different abundance distributions. The northern one is apparently Si+S rich, while the southern one is Fe rich. I find that these knots are moving considerably more rapidly than most of the rest of the remnant, and, in fact, the current expansion rate is consistent with their time-averaged expansion rate, implying that these clumps of ejecta have not been decelerated. This is the first evidence for ejecta "bullets" in the remnant of a Type Ia SN.

ASCA Spectroscopy of Supernova Remnants in the Magellanic Clouds

I. Hayashi[1], **K. Koyama**[1], **J. P. Hughes**[2], **and T. Murakami**[3]

[1]Department of Physics, Kyoto University, Kitashirakawa, Kyoto 606-01, Japan
[2]Harvard-Smithsonian Center for Astrophysics, Cambridge, MA 02138, USA
[3]ISAS, 3-1-1 Yoshinodai, Sagamihara, Kanagawa 229, Japan

We present ASCA results of X-ray spectroscopy of 10 supernova remnants in the Magellanic Clouds. We have derived abundances of the remnants by applying several models taking account of the internal structure of the remnants. These remnants can be divided into three groups according to their ASCA spectral shapes.

Young remnants are clearly classified into Type Ia or Type II origin by their prominent emission lines from medium-Z elements. Type Ia remnants (N103B, 0509-67.5, and 0519-69.0 in the LMC) show over-abundances of elements heavier than silicon, while one Type II remnant (0102-72.3 in the SMC) does so for elements lighter than magnesium.

We have derived mean LMC abundances using several evolved remnants (N23, N49, N63A, N132D, 0453-68.5, and N49B), in which the X-ray emitting gas is considered to be mostly interstellar medium. The abundances are consistent with those from optical data except for silicon and magnesium.